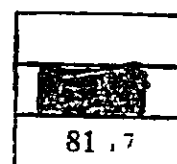


**The Interim Report of
Pre-Feasibility Study on
The Coal Development Project at
The Offshore Area of Zonguldak Coal Field
in The Republic of Turkey**

- Geophysical Study Section -

March 1981

Japan International Cooperation Agency



**The Interim Report of
Pre-Feasibility Study on
The Coal Development Project at
The Offshore Area of Zonguldak Coal Field
in The Republic of Turkey**

- Geophysical Study Section -

 LIBRARY



1051058[4]

March 1981

Japan International Cooperation Agency

国際協力事業団	
受入 月日 '84.5.14	314
登録No. G4421 :	66.7
	MPN

CONTENTS

	Page
I <u>GENERAL</u>	1
1. Objective and Background of the Investigation	1
2. Personnel Constitution	2
3. Contents of Work and Working Period	3
II <u>SUMMARY</u>	5
1. MARINE SEISMIC DATA PROCESSING	5
1-1. Reflection Data Reprocessing	5
1-2. Refraction Analysis	6
2. PROCESSING OF GRAVITY AND MAGNETICS	8
3. OFFSHORE POSITION FIXING	10
4. EVALUATION OF THE GEOPHYSICAL PROSPECTING METHODS	12
III <u>REPROCESSING OF GEOPHYSICAL DATA</u>	15
1. POSITION FIXING IN THE OFFSHORE ZONGULDAK SURVEY	15
1-1. Purpose of the Re-calculation on the Positioning Data	15
1-2. Mapping of the Geophysical Survey Lines	15
1-3. Examination for the Positioning Accuracy	17
2. REPROCESSING OF REFLECTION SEISMIC DATA	19
2-1. Purpose	19
2-2. Method of Reflection Seismic Survey	20
2-3. Field Recording Parameters	23
2-4. Data Processing	24
2-5. Results of the Process	32
2-6. Discussion	32
3. VELOCITY ANALYSIS BY SEISMIC REFRACTION METHOD	35
3-1. Purpose	35
3-2. Principle of Seismic Refraction Method	35
3-3. Procedure of Field Operation	35
3-4. Method of Analysis	35
3-5. Results of the Analysis	40
3-6. Considerations	41

4.	PROCESSING OF GRAVITY AND MAGNETIC DATA	44
4-1.	Purpose	44
4-2.	Survey Method	44
4-3.	Data Processing	44
4-4.	Discussion for Gravity Result	49
4-5.	Discussion for Magnetic Result	50
IV	<u>EXAMINATION OF ACQUIRED RESULTS</u>	55
1.	EXAMINATION OF REFLECTION RESULTS	55
1-1.	Examination Principle	55
1-2.	Velocity Information	56
1-3.	Stack Section	58
2.	EXAMINATION OF REFRACTION RESULTS	63
2-1.	Relation between Seafloor Velocity and Subsurface Topography	63
2-2.	Comparison between Velocity Distribution and Gravity/Magnetics	63
2-3.	Comparison between Analyzed Velocity and Measured Velocity of Rock Samples ..	63
2-4.	Comparison between Velocity Distribution and Geology	65
3.	EXAMINATION OF GRAVITY RESULTS	66
3-1.	Offshore Gravity Survey	66
3-2.	Onland Gravity Survey	66
4.	EXAMINATION OF MAGNETIC RESULTS	68
5.	PROBLEMS AND RECOMMENDATIONS IN POSITION FIXING	69
5-1.	Problems in the Prepared Post-plots	69
5-2.	Recommendations for the Future Offshore Survey	69
6.	GEOLOGICAL AND STRUCTURAL INTERPRETATION IN THE PROJECT AREA ..	71
V	<u>REFERENCES AND LITERATURES</u>	73

LIST OF TABLES AND FIGURES

<u>Table/Figure</u>	<u>Title</u>	<u>Page</u>
Table-1	The adaptability of Geophysical Exploration	13
Table-2	Instruments used for 1978 Seismic Survey M.T.A.	21
Table-3	Statistic of Survey Lines	22
Table-4	Range of Process	22
Table-5	Field Recording Parameters	23
Table-6	List of Stacked Sections	32
Table 7	Field Instrument of Gravity and Magnetic Survey	44
Table-8	Result of Ultra-Sonic Wave Measurement on Rock Samples	64
<hr/>		
Fig. I-1	Illustration of Zonguldak Coal Field (intext)	(in Text)
Fig. III-1-1	Seismic Location and Bathymetry Map	
Fig. III-2-1	Principle of CDP	
Fig. III-2-2	Example of the Effect of Migration	
Fig. III-2-3	Main Processing System	
Fig. III-2-4	Survey Line Map	
Fig. III-2-5	Air Gun & Streamer Cable Towing Array	
Fig. III-2-6	Flow Diagram of Basic Seismic Processing	
Fig. III-2-7	Near Trace Section Line T1-AB (12.5)	
Fig. III-2-8	Near Trace Section Line T2-AB (12.5)	
Fig. III-2-9	Near Trace Section Line T3-AB (12.5)	
Fig. III-2-10	AAC Test Line T1-AB (12.5)	
Fig. III-2-11	Autocorrelogram Line T1-AB (12.5)	
Fig. III-2-12	Autocorrelogram Line T2-AB (12.5)	
Fig. III-2-13	Autocorrelogram Line T3-AB (12.5)	
Fig. III-2-14	Deconvolution and Frequency Analysis Line T2-AB (12.5)	
Fig. III-2-15	Deconvolution and Frequency Analysis Line T1-AB (25)	
Fig. III-2-16	Constant Velocity Scan Line T1-AB (12.5)	
Fig. III-2-17a	Power Spectrum of Near Trace	
Fig. III-2-17b	Power Spectrum of Near Trace	
Fig. III-2-18	Stacking Velocity	
Fig. III-2-19	CVSCAN Line T2-AB (25, CDP-665+666)	
Fig. III-2-20	Velocity Gather Line T1-AB (25), CDP-527	

<u>Table/Figure</u>	<u>Title</u>	
Fig. III-2-21	Possible Reflection Lineups in CDP Trace	
Fig. III-2-22	Stacking Test Line T2-AB (12.5)	
Fig. III-2-23	Velocity Functions	
Fig. III-2-24	Mute Test Line T2-AB (12.5)	
Fig. III-2-25	Post Stack Deconvolution Test	
Fig. III-2-26	Post Stack Deconvolution Test .	
Fig. III-2-27	Post Stack Band Pass Filter Test	
Fig. III-2-28	Wavelet Process Test (1)	
Fig. III-2-29	Wavelet Process Test (2)	
Fig. III-2-30	Wavelet Process Test (3)	
Fig. III-2-31	Plane Wave Simulation Test (CDP 100%)	
Fig. III-2-32	Plane Wave Simulation Test (stack)	
Fig. III-3-1	Example of Seismic Monitor Record	(in Text)
Fig. III-3-2	Explonation of the T-D curve and Velocity Section	(in Text)
Fig. III-3-3	Histogram of the Velocity on Refraction Analysis	(in Text)
Fig. III-4-1	Two-dimensional Horizontal Model	(in Text)
Fig. III-4-2	Principle of Magnetic Analysis on Three-dimensional Prism Model	(in Text)
Fig. III-4-3	Two-dimensional Interpretation using Gravity and Gravity/Magnetic Profiles (A-A')	(in Text)
Fig. III-4-4	Two-dimensional Interpretation using Gravity and Gravity/Magnetic Profiles (B-B)	(in Text)
Fig. III-4-5	Quantitative Interpretation using Magnetic Profile (1)	(in Text)
Fig. III-4-6	Quantitative Interpretation using Magnetic Profile (2)	(in Text)
Fig. IV-1-1	Relations among Basic Data and Displays	
Fig. IV-1-2	Plane View of Basic Section's Alignment	
Fig. IV-1-3	Appearance of Same Reflection Events on Different Types of Display -	
Fig. IV-1-4	An Example of Shot Records	
Fig. IV-1-5	Relation between CDP Velocity and Reflection Dip	
Fig. IV-1-6	Picked Events on Constant Velocity Gather Display (T1-AB(25 m), CDP No.407)	
Fig. IV-1-7	Picked Events on Constant Velocity Gather Display (T1-AB(25 m), CDP No. 527)	
Fig. IV-1-8	Picked Events on Constant Velocity Gather Display (T2-AB(25 m), CDP No. 122)	
Fig. IV-1-9	Picked Value of Comparatively Reliable Events on Constant Velocity Gather Display	

<u>Table/Figure</u>	<u>Title</u>	<u>Page</u>
Fig. IV-1-10	Stacking Velocity Filtering Path Band based on Spread Length	
Fig. IV-1-11	Scanning Velocity Functions with Same NMO Difference Interval	
Fig. IV-1-12	Space-Variant Velocity Functions applied on T1-AB (25 m), CDP No. 48 – 626	
Fig. IV-1-13	Space-Variant Velocity Functions applied on T2-AB (25 m), CDP No. 48 – 712	
Fig. IV-1-14	Typical Example of Seemingly High Velocity Event on Constant Velocity Stack Display	
Fig. IV-2-1	Zoning Map on the Seafloor Features	
Fig. IV-2-2	Distribution of Seafloor-Velocity by Seismic Refraction Analysis	
Fig. IV-2-3	Relation between density and P-wave Velocity	
Fig. IV-3-1	Gravity and Magnetic Map	
Fig. IV-3-2	Residual Gravity Map (Running average method)	
Fig. IV-4-1	Geophysical Profiles Along the Offshore Survey Line	

LIST OF ENCLOSURES

<u>Encl. No.</u>	<u>Title</u>	
1	Interpreted Stack Section	Line T1-AB(25)
2	Interpreted Stack Section	Line T2-AB(25)
3	Interpreted Stack Section	Line T1-AB(12.5)
4	Interpreted Stack Section	Line T2-AB(12.5)
5	Interpreted Stack Section	Line T3-AB(12.5)
6	24-fold Record Section	Line T1-AB(12.5)
7	24-fold Record Section	Line T2-AB(12.5)
8	24-fold Record Section	Line T3-AB(12.5)
9	Time Migrated Section	Line T1-AB(12.5)
10	Time Migrated Section	Line T2-AB(12.5)
11	Time Migrated Section	Line T3-AB(12.5)
12	Depth Migrated Section	Line T1-AB(12.5)
13	Depth Migrated Section	Line T2-AB(12.5)
14	Depth Migrated Section	Line T3-AB(12.5)
15	24-fold Record Section	Line T1-AB(25)
16	24-fold (Record Section (for 8 functions)	Line T1-AB(25)
17	24-fold Record Section	Line T2-AB(25)
18	Time-Distance Curve and Velocity Section	Line T1-AB(12.5)
19	Time-Distance Curve and Velocity Section	Line T1-AB(25)
20	Time-Distance Curve and Velocity Section	Line T2-AB(12.5)
21	Time-Distance Curve and Velocity Section	Line T3-AB(12.5)

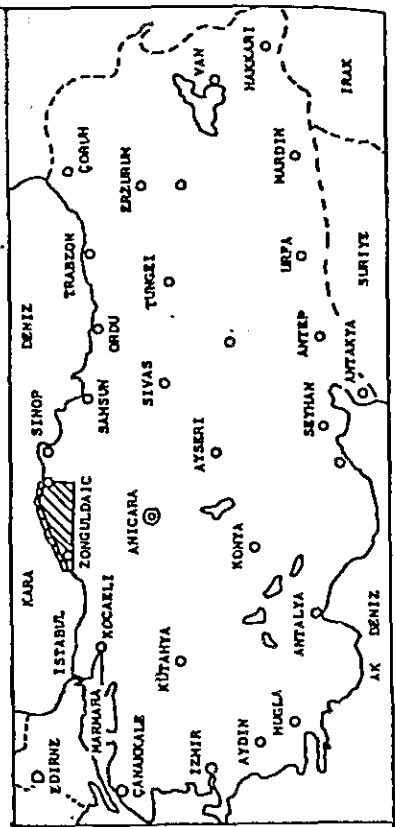
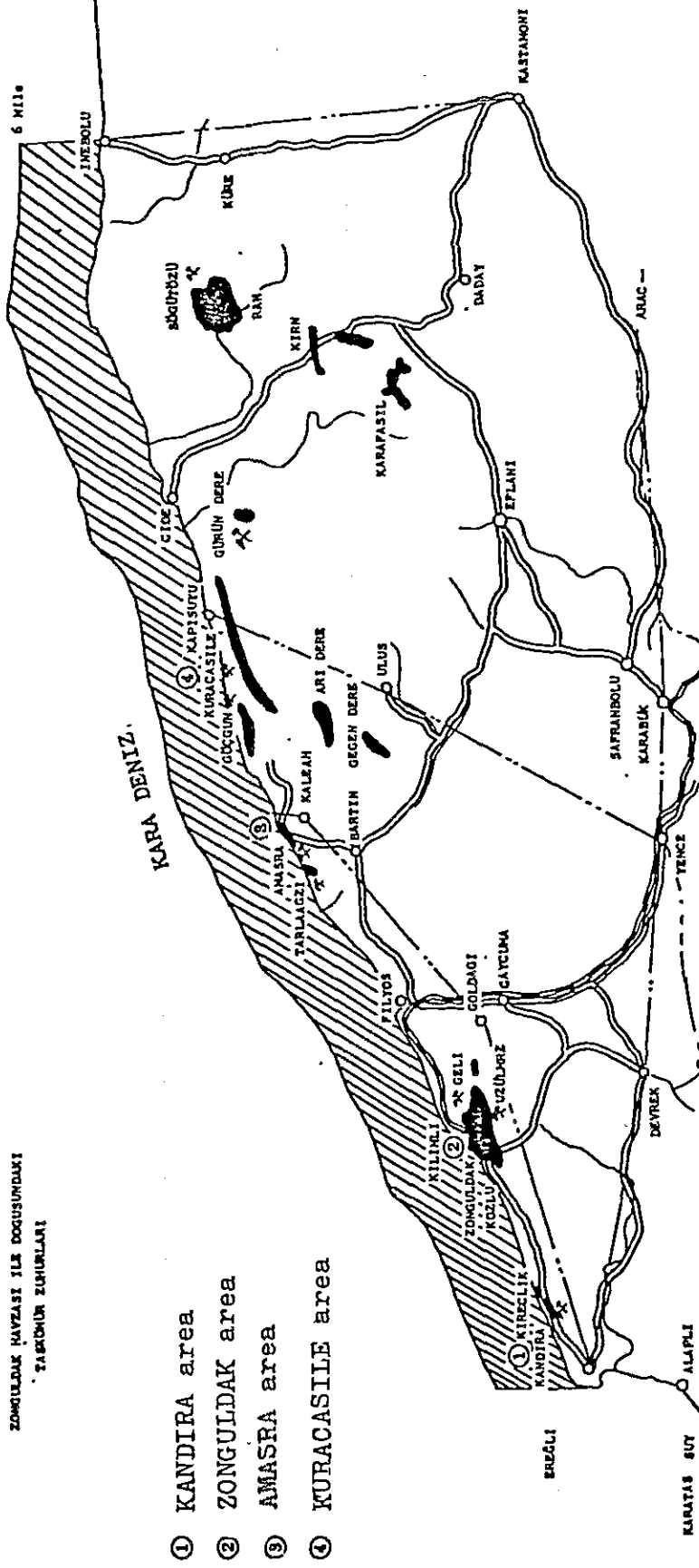
I. GENERAL



Fig. I-1 Illustration of Zonguldak Coal Field

ZONGULDAK HAVZASI İLE DOĞUSUNDAKİ TAŞKÖMÜR ZUHURLARI

- ① KANDIRA area
- ② ZONGULDAK area
- ③ AMASRA area
- ④ KURACASILE area



17.1.1926 Tarih Ve 289 Sayılı Teşkeri maddesiyle tevbitt edilen 1293 hüdudü.
 5.2.958 tarih Ve 4/9925 Sayılı Kararı ile E. K. İ. İ. ye devredilen hüdudü.
 3.12.953 tarih Ve 4/1922 Sayılı Kararı ile tevbitt edilen İaletime hüdudü.
 Tevbitt sahaları

TEVSI SAHASININ
 KIZIL KIRIS 'DAGI

KIZIL KIRIS 'DAGI

17.1.1926 Tarih Ve 289 Sayılı Teşkeri maddesiyle tevbitt edilen 1293 hüdudü.
 5.2.958 tarih Ve 4/9925 Sayılı Kararı ile E. K. İ. İ. ye devredilen hüdudü.
 3.12.953 tarih Ve 4/1922 Sayılı Kararı ile tevbitt edilen İaletime hüdudü.
 Tevbitt sahaları

TEVSI SAHASININ
 KIZIL KIRIS 'DAGI

KIZIL KIRIS 'DAGI

KIZIL KIRIS 'DAGI

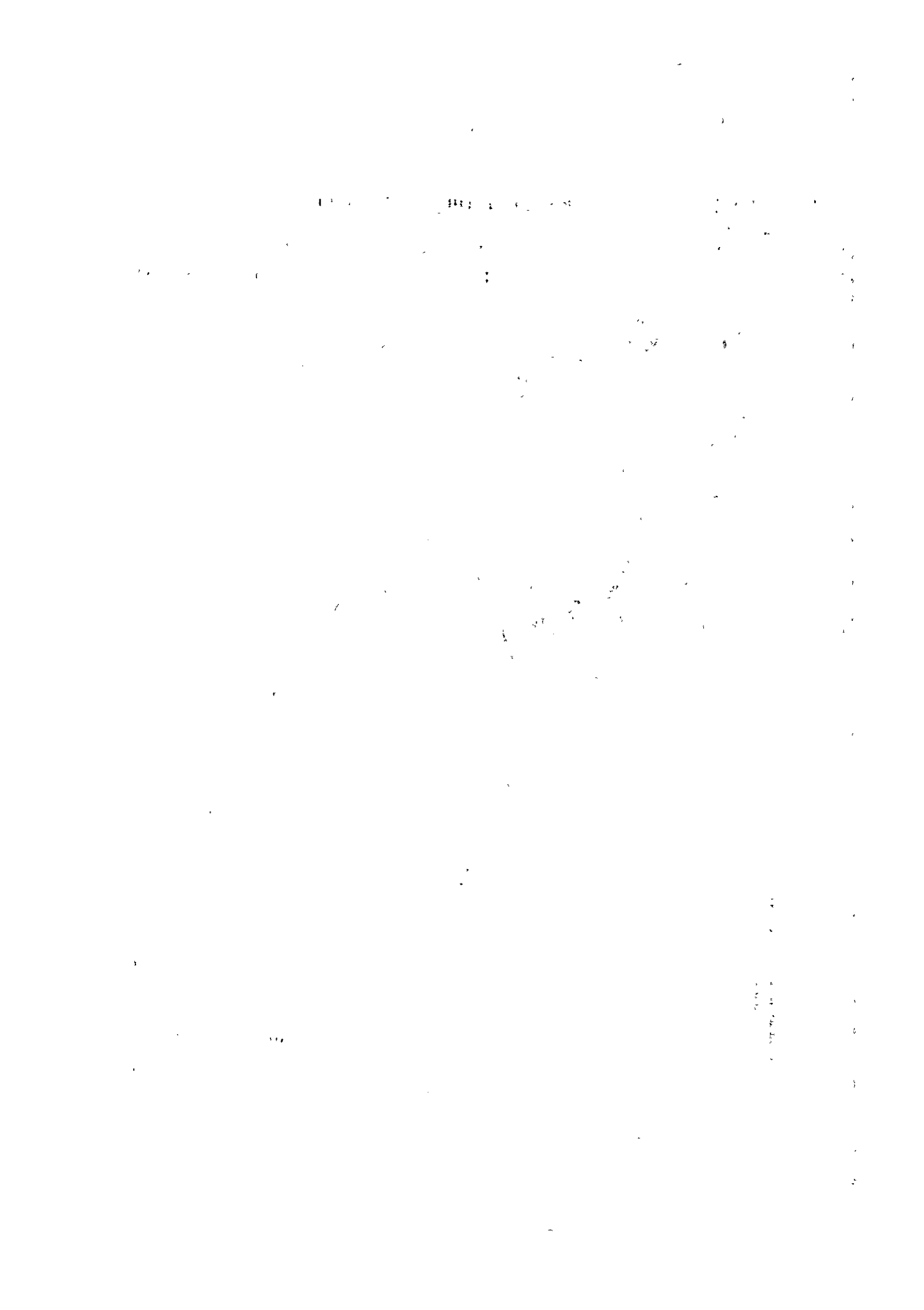
17.1.1926 Tarih Ve 289 Sayılı Teşkeri maddesiyle tevbitt edilen 1293 hüdudü.
 5.2.958 tarih Ve 4/9925 Sayılı Kararı ile E. K. İ. İ. ye devredilen hüdudü.
 3.12.953 tarih Ve 4/1922 Sayılı Kararı ile tevbitt edilen İaletime hüdudü.
 Tevbitt sahaları

TEVSI SAHASININ
 KIZIL KIRIS 'DAGI

KIZIL KIRIS 'DAGI

0 10 20 30 40 50 KM

ÖLÇEK: 1-1.000.000



I. GENERAL

1. OBJECTIVE AND BACKGROUND OF THE INVESTIGATION

An experimental operation of four seismic reflection survey lines, a total of 37.6 km long, was carried out in June, 1979, by the Maden Tetkik ve Arama Enstitüsü (hereafter called M.T.A.)*¹ as a link in the chain of the Offshore Zonguldak Coal Mine Exploration Project at offshore Zonguldak coal field located in the northwestern part of the Republic of Turkey.

In the meantime, the Preliminary Survey Mission despatched from the Japan International Cooperation Agency (hereinafter called JICA) examined the results of this experimental operation, such as field technique, data processing and data analysis, etc., and reached to the conclusion that there is a necessity of reprocessing and reanalysis with those data in order to improve their quality.

In accordance with the aforementioned judgment and also based on the 'Scope of the Works' (hereinafter called S/W) signed between the Türkiye Kömür İşletmeleri Kurumu (hereinafter called T.K.İ.)*² and the Preliminary Survey Mission from JICA in February, 1980, the restudy of the abovementioned data and the training of the two geophysicists from the M.T.A. were carried out in Japan under the following objectives:

- 1) To attempt the quality implementation of seismic reflection record sections in Japan by reprocessing and reanalyzing the seismic reflection data obtained from the experimental operation at offshore Zonguldak coal field;
- 2) To obtain a relative relation between the geological formation and the estimated rock facies inferred from the seismic velocity acquired from the seismic reflection record by using refraction technique;
- 3) To accept and train two trainees from the Turkish government in order to strengthen and bring up ability and number of geophysicist, who has to be able to guide the whole offshore geophysical exploration in the Turkey, by providing training not only with the analyses of seismic data but also with the synthetic analysis and interpretation of all available data including offshore gravity survey and magnetic survey.

This is a report presenting the total results of this restudy works and the further cooperative program has to be made based on the results of this reprocessing and restudy works.

Note: *1: M.T.A. — Mineral Research & Exploration Institute of Turkey in English.
*2: T.K.İ. — Turkish Coal Enterprise in English.

2. **PERSONNEL CONSTITUTION**

The member involved in this project is as follows:

NAME OF EXPERT	DUTIES	
	FOR ANALYTICAL WORKS	FOR TECHNICAL TRAINING
MASAAKI INOUE	Team Leader (Geology)	—
TAKUYA KAMETANI	Geophysical Exploration (Processing of Reflection data)	Reflection Method
YUTAKA AOKI	Ditto. (Ditto)	Ditto.
HIROSUKE OHBAYASHI	Ditto. (Analysis of Refraction Data)	Refraction Method
OSAMU NAKANO	Ditto. (Ditto)	Ditto.
KUNUYUKI KATAYOSE	Ditto. (Analysis of Gravity & Magnetism)	Gravity & Magnetic Exploration
MASAHIRO TAKEMORI	Ditto. (Ditto)	Gravity & Magnetic Exploration, Positioning
KIYOSHI MORI	—	Reflection Method

The members listed above carried out the all geophysical studies together with the belowmentioned two counterpart geophysicists being abroad to Japan as a JICA participant from Turkish government.

Note: The participants from the geophysics department of M.T.A. in Republic of Turkey who are invited by JICA are:

Mr. Kenan Eres (Chief Engineer of Geophysics)

Mr. Sinan Kavukcu (Geophysical Engineer)

3. CONTENTS OF WORK AND WORKING PERIOD

3-1 Analysis Works (From October 11, 1980 to March 31, 1981)

- a) Computer Processing of Reflection Data (Reprocessing)
- b) Analysis by Refraction Method
- c) Investigations of Gravity and Magnetic Exploration Data
- d) Review of Positioning Data

3-2 Technical Training of Turkish Geophysicist (From October 12 to December 21, 1980)

Mr. S. Kavukçu: Arrived on October 12 and left on December 21, 1980.

Mr. K. Eres: Arrived on October 26 and left on December 21, 1980.

Main Curriculum of the participant Computer Processing of Reflection Data, Analysis of Refraction Data, Qualitative and Quantitative Analyses of Gravity and Magnetic Data and Positioning, etc.

Supplementary ones: Inspection of Geological and Geophysical Survey Boats, such as Hakurei-maru and Kaiyoh-maru, etc.

II. SUMMARY



II. SUMMARY

1. MARINE SEISMIC DATA PROCESSING

1-1 Reflection Data Processing

Results obtained from this data processing indicate that data acquired by using long streamer cable (length of active section: 1.2 km) are better than data by using short streamer cable (length of active section: 0.6 km). Long spread data are:

- a) More reliable concerning to their velocity information;
- b) Showing their lineups more characteristically, based on better stacking velocity resolution. Because NMO (normal moveout) correction on long spread for same velocity function has to be three to four times larger than short spread.

Therefore, after taking long spread informations as a general guide, and deeming that lineups on short spread being concordant with above informations should be more reliable, these processing and interpretation were carried out. Especially stacking velocities applied on all lines were designed mainly on velocity informations acquired on long spread, and as a result no contradiction of velocity analysis between long and short spread is generally observed. In general, events considered as a true reflection dip seawards; this phenomenon is not discrepant with the sparker's results in the offshore Kozlu (Hosono et al, 1970). Probable to possible terrace and a small culmination (seems to be local reverse dip associated with fault) were observed in the section of the line T1-AB (25 m). This processing was aimed primarily on getting better technical guide line, on which the decision on continuing further geological survey can be made, and with which the improvement of survey specifications will be designed when further survey may be planned. Therefore, resources were allocated to get basic data and informations for establishing this guide line, and insufficiency for clarifying geological details resulted inevitably. It will be hoped to conduct supplemental reprocessing for more detail informations and restart the field survey with improved methods for more comprehensive geological study.

Picked events on time sections as preliminary results are shown on Encl. 1, 2, 3, 4 and 5. Black dots at very shallow portion show sea bottom reflection time of echo sounder records. Shallowest almost flat events show stacked energy of sea bottom refraction, but do not mean the sea bottom itself exactly, because NMO correction was not made for refraction but reflection, and the assumed velocity was different from that of water. However, the writers wanted to show approximate water depth and sea bed configurations by these

events. Hatchings on the sections of T2-AB (25 m) and T2-AB (12.5 m) indicate disturbed portions by diffraction type noise. Almost events were picked on final stack sections, but events marked with VD, for instance, were picked on the stack section of velocity VD. No indications of certainty and accuracy were attempted because of poor quality. Solid and broken lines may express some nuance, but quite subjective.

1-2 Refraction Analysis

The results of refraction analysis are summarized as follows:

- A) Strictly speaking, the geological interpretation of the offshore seismic data based on the refraction analysis is quite difficult and also be fairly subjective owing to insufficient amount of data. The estimation of the seafloor characteristics was made by assuming rock facies from the seismic velocities calculated from the first arrivals recorded on the monitor records.
- B) However, there is a possibility to improve the results of further studies for acquiring a more reliable geological interpretation by carrying out the following:
 - a) Velocity measurement of rock samples in laboratory,
 - b) Refraction analysis in the appropriate onland area,
 - c) Well shooting in the coal bearing and associated formations,
 - d) Additional surveys with an appropriate line spacing in the offshore project area.
- C) Calculated velocities of the uppermost layer below sea bottom by the refraction method range from 2.5 to 5.6 km/sec., of which 60% ranges from 3.6 to 4.0 km/sec.
- D) There are comparatively good relations between the calculated velocities and the seafloor topography. And also some correlations between the calculated velocities and the other geophysical events were observed as mentioned below:
 - 1) Topography: A large variation in the velocity is observed in the area along the coast where the sea bottom inclines toward the offshore with a dip of 2 to 3 degree, while a relatively constant velocity is obtained at the flat sea bottom area implying the existence of a homogeneous sediment.
 - 2) Gravity: In the area west of Zonguldak, a relatively high velocity occurs in the high gravity area. It suggests the existence of high density materials in the shallow part immediately below sea bottom. A couple of comparatively low velocity areas exists on the gravitationally steep slope zone in the west-northwest of Zonguldak. It may represent the existence of fault or fault zone.
 - 3) Magnetics: The obvious magnetic anomalies identified on the lines, T1 (12.5 m), T2 (12.5 m) and T3 (12.5 m), respectively, appear to suggest a zone parallel to

the coast and this assumed zone seems to coincide the area where the homogeneous velocity ranging from 3.6 to 4.0 km/sec. is observed.

- 4) Velocity of The Rock Samples: Since the velocity of limestones of the Apsien and Barremien series was more than 6.3 km/sec., the high velocity medium described in the above 2) may suggest the existence of limestone outcrops which would be the extensions of the limestones exposed nearby onland at the west of Zonguldak. On the other hand, the velocities of sandstone and volcanic rock are significantly lower than that of limestone. The moderate velocities distributing in the offshore area may suggest the development of sandstones or volcanic rocks.
- E) Based on the characters of the time-distance curves, the followings will be considered:
- 1) There is a possibility that the sediments in the objective area seem to be covered by the younger sediments, possibly Quaternary ones, in some places. On the other hand, there seems to be a possible Cretaceous limestone exposure at the western offshore of Zonguldak.
 - 2) It is difficult to estimate the layered structure below seafloor by refraction analysis since the refracted arrivals only from the sea bottom were recognized.
 - 3) The results of calculations suggest that there are two possible cases, by which the time-distance curve can be explained, of the underlying layers below sea bottom, such as one is an existence of one homogeneous thick layer more than 150 m thick and the other is a combination of two layers consisting of a high velocity layer and an underlying low velocity layer.
 - 4) The maximum applicable water depth for the refraction method is 200 meters or 100 meters for the long or the short streamer cable respectively.
 - 5) To use the previous seismic records of 1977 or 1978 lines is recommendable since the analysis of these data may lead to a better understanding for the correlation between velocity and lithology.

2. PROCESSING OF GRAVITY AND MAGNETICS

Since the total amount of offshore gravity and magnetic data was not sufficient enough to make a detailed geological interpretation, the previously acquired onland data had to be interpreted. Taking these onland data into account, the adaptability of gravity and magnetic methods is appraised to the future exploration in the offshore Zonguldak coal field. The final results obtained by gravity and magnetic methods affect indirectly to the geological interpretation mutually. However, it has been concluded that if these data are carefully interpreted in combination with offshore seismic data, the gravity and the magnetics may contribute on establishing bounds on correlation and may provide lithologic informations in the future offshore exploration. The main points we could clarify by gravity and magnetic methods are as follows:

A) Gravity Method

Concerning the Bouguer gravity map, since it is a combination of shallow, intermediate and regional anomalies, a specific frequency component of anomalies, which was considered to be indicative of geologically interesting sources, was extracted by means of "Running average method" which is one of qualitative analysis to obtain a residual gravity map. As a result, it was found that this "Running average method" will be effective on outlining the position of local anomalies.

Some of the positive anomalies thus obtained on the residual anomaly map coincide with the Palaeozoic high and on the other hand, some of the relative low seem to coincide with the area where a sedimentary basin exists at the east of Zonguldak. Furthermore, it was obvious that the indication of faults on the residual gravity map is much clearer than that on the Bouguer anomaly map. These results imply that the gravity method can provide an important information in delineating the lower Palaeozoic structure. In the Zonguldak area, the density contrast between each lithologic unit is reportedly small although that is a fundamental factor controlling gravitational anomaly. To confirm this, the density measurement by using rock specimen will give some helps for the establishment of the future exploration programme.

B) Magnetic Method

Generally, the magnetic method is considered as one of the effective method for detecting tuff and volcanic materials. As a matter of fact that the locations of the magnetic anomalies, observed in the onland area, coincides with the distribution of the

volcanic formations in the adjacent area of Zonguldak coal field.

In the offshore area, on the other hand, the observed magnetic anomalies seems to have some relation between the seismic velocity. The further data acquisition in the offshore area will be recommended to obtain a complete magnetic map which lead to a better understanding on interpreting overall geophysical data.

3. OFFSHORE POSITION FIXING

A post-plot map, namely a survey line map, was provided by M.T.A. as the base map for the reprocessing in the geophysical survey of the offshore Zonguldak. However, the interval of the post-plot was wide and partly inconstant according to the results shown on the map. And the map projection systems were not united between the offshore and onland map making. It was, therefore, considered that these conditions might affect to the forthcoming geophysical interpretations. The recalculation and the re-mapping for the post-plots are thus carried out in Japan. Furthermore, the consideration is made for the positioning accuracy of the Integrated Navigation System which was used during this survey, and the examination is made for the post-mission data processing.

The followings are the results of the examination and the recommendations for the future offshore exploration survey.

A) Results of The Examination

- 1) The offshore position fixing, based on the Integrated Navigation System, is generally operated according to the following procedures, such as a) to determine the ship's reference position by the satellite update technique at the running-in per survey line, and b) the locations of the subsequent shotpoints are calculated by accumulating the ship's horizontal movement against the sea bottom, which is customarily accomplished by the Doppler-Sonar's deadreckoning method between the satellite updates. Therefore, the accuracy of the subsequent ship's position is strongly dependent on the reliability and the frequency of the satellite updates. On the other hand, it appears to be considered that the insufficient satellite updates were made during the line shooting in this field survey. The Integrated Navigation System was individually operated as the primary positioning system instead of any other high accurate radio navigation system. Under these circumstances, the final positioning accuracy in this survey may have some considerable errors as for the purpose of the offshore geophysical survey.
- 2) Particularly, the reliability of the position fix at the start of each line seems to be not too high. And at the west end of the T2 line where the sea bottom feature is rough and steep, it is suspected an existence of a cumulative error in the Doppler-Sonar's dead-reckoning.
- 3) This is simultaneously suggested that the gravity errors on the Eötvös correction is used to be relating to the horizontal vector component of the ship.

- 4) Furthermore, it is observed the inconstant interval of the subsequent shot points had been occurred in some portions of the line. It may diminish the stacking effect for amplifying true reflection signals.
- 5) The comparison between the published bathymetric map and the sounding records in this survey did not give any assuredness with the position certainty of the present survey.
- 6) The useful base map has been drawn up by using the recalculated post-plots. After uniforming the map projection system with the onland and the offshore maps, the direct compilation became possible with the both maps.

B) Recommendations for The Future Offshore Survey

- 1) The primary positioning system shall be based on the highly accurate radio navigation system, which shall carefully be calibrated in accordance with the advance of the survey.
- 2) In any case, a strict log shall be kept and the onboard quality control shall regularly be maintained.
- 3) The Integrated Navigation System shall be used as the back-up positioning system.
- 4) The line control on board shall be made according to a preplot (ref. IV-5.2.), and if available, the use of Track plotter (ref. IV-5.2.) is highly recommendable.
- 5) Immediately after the survey, the post-plot calculation shall be made and be recorded onto the magnetic tapefile, which includes the continuous file updates.
- 6) Simultaneously, the seismic location map shall regularly be draughted using the update post-plot file.
- 7) The post-plot map seems to obtain better outcome when it is projected upon the U.T.M. map projection system.
- 8) The geophysical survey line must be programmed to have some traverse lines.
- 9) The calibration of the echo-sounding system shall be carried out in the project area ahead of the survey.

4. EVALUATION OF THE GEOPHYSICAL PROSPECTING METHODS

Although, at the preliminary stage, a definite evaluation of adaptability of the geophysical method as a tool for the future exploration activities is somewhat difficult due to an insufficiency of data acquired so far, the present studies lead a several interesting results which suggest the effectiveness of the seismic method combined with gravity and magnetic survey.

It is believed that a successful result can be expected if further efforts is made to acquire the additional offshore data as well as velocity information with various rock specimen. Further investigation on the improvement of quality of the existing seismic system is also considered to be important.

The following Table 1. shows the adaptability of the geophysical methods and problems involved.

Problems to be Solved

Geophysical Methods	Countermeasures
Seismic Reflection Method	<p>improve quality of data on acquisition stage: a) Control of source spectrum; b) Control of energy; c) Review of airgun array; d) Review length of streamer cable, etc.</p> <p>improvement of data processing.</p> <p>positioning of seismic velocity data of rocks.</p> <p>velocity measurement of the core and sonic log in the boring hole if possible)</p>
Seismic Refraction Method	<p>improve the accuracy on positioning.</p> <p>develop the new method for recording core-log and opposite seismic records.</p> <p>correlation data between velocity and rocks: a) velocity measurement of rock samples; b) Well logging; c) Test operation of refraction method in the field area.</p>
Gravity Survey	<p>it is necessary to establish a mutual relation between geology and gravitational survey results.</p> <p>utilize the results of qualitative analysis obtained by the running average method to the interpretation of geological structure.</p> <p>velocity property measurement of rock samples, correlation of boring data, increase of quantity on exploration.</p> <p>improvement of positioning accuracy. (Use of trisponder)</p>
Magnetic Survey	<p>improvement and measurement of physical properties of rocks.</p> <p>increase of quantity on exploration.</p> <p>improvement of correspondability to the other survey.</p>

Table 1: The Adaptability of Geophysical Exploration for The Development of The Offshore Zonguldak Coal Field and its Problems to be Solved

Geophysical Methods	Adaptability	Problems	Countermeasures
Seismic Reflection Method	<ol style="list-style-type: none"> 1) To be able to infer the tendency of reflection plane (For example: As same as results of Speaker survey at offshore Kozlu in 1970 and also that of gravity survey. 2) To be able to recognize a terrace and a small anticlinal structure in the reflection profile. 	<ol style="list-style-type: none"> 1) Detection of the primary reflection is insufficient at the moment due to: a) geological structure does not have visible primary reflection; b) amplitude of refracted wave, multiples and primary reflection is too big. 2) Processing capacity of M.T.A. computer and details of software are unknown. 3) On acquiring back data for velocity assumption 	<ol style="list-style-type: none"> 1) To improve quality of data on acquisition stage: a) Control of source spectrum; b) Control of source energy; c) Review of airgun array; d) Review of length of streamer cable, etc. 2) Review of data processing. 3) Acquisition of seismic velocity data of rocks. (P-velocity measurement of the core and sonic survey in the boring hole if possible)
Seismic Refraction Method	<ol style="list-style-type: none"> 1) There is a possibility to assume rock facies at seafloor by estimating seismic velocity from the reflection seismogram. 2) Refraction analysis will be conducted as a two layers structure of sea water and seafloor within a depth range less than 150 or 200 m. 3) It will be able to obtain a sufficient velocity data to judge the rock facies and also a low velocity zone possibly caused by fault or disturbed zone when the dip of seafloor is less than several degrees. 	<ol style="list-style-type: none"> 1) There is a possibility of errors in the velocity analysis data due to the one way transit time analysis. 2) As the basic data on correlating seismic velocity and corresponding rock facies, the interpretation of velocity analysis is not clear. 	<ol style="list-style-type: none"> 1) To improve the accuracy on positioning. 2) To develop the new method for recording corresponding opposite seismic records. 3) For correlation data between velocity and rocks: a) P-velocity measurement of rock samples; b) Well shooting; c) Test operation of refraction method on land area.
Gravity Survey	<ol style="list-style-type: none"> 1) It is effective for general geological structure survey as a reconnaissance or preliminary survey. 2) It will be a fundamental data to estimate the geological structure of Lower Palaeozoic System and the coal bearing formations surrounded by the Lower Palaeozoic System based on the residual gravity analysis. 3) There are good correspondence both between the high gravity area and the high seismic velocity area of refraction analysis and between the low seismic velocity zone and the steep dipping area on gravity contour. 4) The gravitational steep dipping area may correspond to the fault zone. 	<ol style="list-style-type: none"> 1) A caution will be required for analysis and interpretation of data because no visible gravitational difference between rocks of Cretaceous and Palaeozoic. 2) To review the correspondence between the coal mine locations and the gravitational basin by residual gravity. 	<ol style="list-style-type: none"> 1) It is necessary to establish a mutual relation between geology and gravitational survey results. 2) To utilize the results of qualitative analysis obtained from the running average method to the interpretation of geological structure. 3) Physical property measurement of rock samples, study of boring data, increase of quantity on exploration. 4) Increase of positioning accuracy. (Use of trisponder together)
Magnetic Survey	<ol style="list-style-type: none"> 1) There is a good correspondence between the magnetic anomaly of the magnetic total intensity and the estimated distribution of the cretaceous volcanic and tuffaceous formations. 2) It will be possible to estimate the existence of the magnetic body by adopting magnetic quantitative method. 3) The magnetic anomaly appears to correspond to the area having the seismic velocity of 3.6 ~ 4.0 km/sec. 	<ol style="list-style-type: none"> 1) Correspondability for the other geophysical exploration is uncertain. 2) There is a few data for interpretation of correspondability between gravitcal anomaly, low seismic velocity area and relative low density area. 	<ol style="list-style-type: none"> 1) Study and measurement of physical properties of rocks. 2) Increase of quantity on exploration. 3) Study of correspondability to the other survey results.

III. REPROCESSING OF GEOPHYSICAL DATA

.

.



III. REPROCESSING OF GEOPHYSICAL DATA

1. POSITION FIXING IN THE OFFSHORE ZONGULDAK SURVEY

1-1 Purpose of the Re-calculation on the Positioning Data

The location map of the geophysical survey lines in the offshore Zonguldak coal field is provided by M.T.A. on the scale of 1:25,000. However, the interval of each point which describes the ship's position (hereafter the 'post-plot') was too wide and also inconstant in some portions of each line. It will be considered that some probable errors could occur in the postmission data processing or the plotting. And the map projection system does not coincide in the offshore and onshore map making.

Since these conditions may affect for carrying out forthcoming geophysical interpretations, the navigational data were, therefore, re-processed. And then a new location map has been prepared based on the re-calculated seismic locations.

1-2 Mapping of the Geophysical Survey Lines

1-2-1 Map projection system

To describe offshore geophysical survey lines, the Mercator projection system for map making has been generally employed at M.T.A., and it is conventionally utilized for the marine chart mapping in the world. However, it can be said that this Mercator projection system is inconvenient for the map of the offshore geophysical survey in the area of middle-high latitude, because the distance between two datum points is not always given in the same length depending on the location of the map. For the onland mapping, on the other hand, the Transverse Mercator projection (T.M. projection) system is used at M.T.A. for topographic and geological mapping. The coast line, in principle, does not coincide in the different map projection. Furthermore, as the coal bearing field may be existing more than 100 kilometers along the Black Sea coast, the active offshore exploration survey will be held much more in the future. It is considered that the Universal Transverse Mercator projection (U.T.M. projection) system is the most adequate one as the base map for geophysical activities in this field. In this system, the Y-axis or X-axis of the rectangular coordinates are the equator or the meridian of 33 degree E respectively in this area. The zone for the three degrees in each side of the central meridian can be projected on the plane, map on which they will be shown as a area, which is about 500 kilometers wide in the west or east of it in one plane.

After applying this system, it allows to connect the onland geological map and the offshore map directly without any significant discrepancies, and more the post-plotting in the future offshore survey can be overlaid accurately.

1-2-2 Post-plot calculations

The post-plot for the ship's position is calculated by using the print-out of onboard navigation log according to the following procedures:

STEP-1: To shift the datum of geographical coordinates to International ellipsoid (standard in Turkey) from WGS-72 ellipsoid (NNSS satellite's). By lacking of detail information with navigation logs, the geographical coordinates on the lists are recognized as the positions based on the satellite's ellipsoid.

STEP-2: To convert the coordinates to U.T.M. rectangular system from geographical coordinates.

Latitude (deg. min. sec.) → Northing : X (m)

Longitude (deg. min. sec.) → Easting : Y (m)

STEP-3: To step-back the ship's position (the satellite antenna position) into the common depth point. In this survey, every C.D.P. point is referred to each air-gun position based on the Turkey's standard. In Japan, however, the C.D.P. point is usually referred to the center between the air gun and the nearest hydrophone group.

1-2-3 Seismic location map

The post-plot calculations are carried out on every 24 shots for the short cable line, and every 12 shots for the long cable line respectively. This means that every calculation was made at every 300 meters interval on each live by using i.e. every 300 meters each line, using HP-97 hand carriable calculator. These locations are draughted in the seismic location map with bathymetric contours as shown in Fig. III-1-1. In this map, the short cable lines, T1, T2 and T3, are displayed with solid lines, and the long cable ones are displayed with broken lines.

The T2 lines (both short and long cable) are similarly run in the map, because the each individual survey was planned to compare each seismic result. Notwithstanding the T1 line was also planned under the same reason, the short cable line and the long cable line were separately located. A satellite update in the long cable T1 line has been made at right beginning on the start, the update in distance was very large at that moment. The line separation might be occurred by this navigational reason, but no significant errors would be included in the real time positioning result. For post-plot recalculations, reasonable records

are picked up and doubtful ones are omitted. Then some portions of a line are unmapped particularly in the beginning of each line. The seismic location map is used as the base map for all the geophysical interpretations.

1-3 Examination for the Positioning Accuracy

The final examination for the positioning accuracy was entirely difficult due to the independent operation of the Integrated Navigation System which was not supported by any high accurate radio navigation system. In general, however, the statistical error of the system is usually represented by a circle of 100 meters radius under 80% probability when the system is operated carefully (references (14), (15)).

Since the geophysical lines in this survey are located near the coast, the position confirmation could have been made by the radar observation or any other method (it is not sure what was really carried out at that time). Considering these conditions, the extent of average error can be expected to be smaller than the abovementioned circle.

It is another useful method to check the ship's position accuracy by comparing with the published bathymetric map. In the area of offshore Zonguldak, two bathymetric maps are available, the one is Kozlu - Zonguldak (Hidrografi Dairenden, 19-) and the other is Offshore Kozlu (Nittetsu Mining Consultant Co. 1970). These bathymetric maps are shown in Fig. III-1-1. The echo-sounding data of the present survey lines do not exactly coincide with those of bathymetric maps, the considerable reasons of the abovementioned discrepancy are;

- 1) By the poor positioning accuracy on the early surveys.
- 2) By the poor sounding accuracy in the present survey (it may be caused by an insufficient calibration for the sounding system).

Therefore, the positioning accuracy of the present survey could not be verified by this way.

The position fixing in the offshore geophysical exploration is occasionally apt to be a down graded technique compare with geophysical data acquisitions'. But it should be maintained to meet the adequate accuracy for the proposed geophysical exploration. Incorrect and/or uncertain position measurements may sometime severely affect to the quality of geophysical data. For instance, a) In the seismic reflection analysis, inconstant spacing of the subsequent shots may produce the various problems on the C.D.P. stacking. b) In the refraction method, inaccurate position of each shot point may decrease the reliability of the calculated velocity. c) In the ship-borne gravity measurements, the erroneous position fix will build

up an inaccurate ship's velocity which may change the Eötvös correction. One milligal of the correction can easily be given by the failures of 0.2 knots on the speed, or of 2 degrees on the ship's heading.

On using the Integrated Navigation System as a primary positioning purpose for the offshore geophysical survey, the above attentions must practically be taken into account. As the system is heavily dependent on the satellite update technique, the reliability of the update ship's position strongly affects to determination of the subsequent shot point locations. The under the conditions, such as ship's turn before satellite updates or in the deep sea (deeper than 200 meters), may usually increase cumulative errors on deadreckoning of the Doppler Sonar system, so that these generally diminish the reliability of the position fix. In this survey, the satellite updates have not been made on T2 line (both long and short cables), it might be necessary to consider for the gravity interpretation.

2. REPROCESSING OF REFLECTION SEISMIC DATA

2-1 Purpose

The purpose of reprocess of the reflection seismic data, which was recorded by MTA using the R/V SISMIK-1, is to clarify various technical problems and to study appropriate seismic exploration method for future coal exploration work in the area of offshore Zonguldak, Republic of Turkey. The survey is attempted to investigate possible extension of the onshore Zonguldak coal field to offshore area. In 1978, first multichannel air gun seismic survey was carried out by MTA for this purpose (Kavukçu, 1979). During the survey both air gun and sparker were tested as a energy source varing some of shooting and recording parameters. Despite these efforts, strong multiple signal and diffraction masked primary reflection and thus underground structure. This phenomena, strong multiple and diffraction caused by high velocity carbonate of Cretacious age, had been observed in the geophysical survey by Nittetsu-Mining Consultants and Ito-Chu Corporation in 1970, and also recognized in the oil exploration work by MTA in 1977. On these accounts, another high resolution seismic survey was attempted in 1979 by MTA adopting short streamer cable of 600 m, short offset, small air gun volume and high sampling rate to avoid multiple signals. This data was processed extensively at MTA's data processing center using TIMAP 980-B and MATE-500 software package. However some kind of difficulties namely strong multiple and poor primary reflection, are encountered again and further efforts to make seismic information reliable have been desired.

On the other hand, Japan International Cooperation Agency (JICA) which has been keeping contact with the Republic of Turkey, send two specialists to Turkey in 1979 and another party of five in 1980 to review all of the available geological/geophysical data including seismic record and to establish future exploration and development work in the Zonguldak coal field. It was concluded through their investigation that reprocessing of some of 1979 data would be necessary to study detailes of the problems. Consequently it was decided to reprocess three lines of totally 22.3 km and those data were sent to JICA with two other longer cable (1200 m) seismic lines. According to the report of 1980 JICA mission, longer deconvolution operator and higher stacking velocities than those in MTA processing were recommended. In addition to these points, various attention were recommended to be paid to attenuate multiples and recover primary reflections.

2-2 Method of reflection seismic survey

2-2-1 Principle of reflection method

The object of reflection seismic method is to make geological vertical profile by means of artificial seismic signals. Since each sedimentary layer has its own acoustic characteristics, seismic wave is reflected at the boundary of two acoustically different layers. Therefore, it is possible to know the existence of the boundary, by shooting dynamite or other equivalent energy source and receiving reflected seismic wave, at the depth corresponding to the half of the traveltime. This principle is exactly the same with echo. If shooting and recording is repeated along a line on the surface, underground structure may be revealed by the analysis of reflected seismic wave.

The concept is very simple but actual survey and data manipulation is somewhat complicated. This complexity is associated with non-zero offset shooting and multichannel data recording.

In contrast to those single channel acoustic survey such as so called profiler, seismic wave velocity information can be obtained from multichannel data and it is used in succeeding stacking process. The basic concept of this method is the CDP (=Common Depth Point).

In Fig. III-2-1, S and P represent shot point and receiver point respectively. Suffix denotes different shot or receiver point. If structure is assumed as horizontal two layer type, then raypaths shown by solid line and arrow have same reflection point D. Accordingly, seismic records which travelled along S1-D-P1, S2-D-P2, S6-D-P6, are called CDP traces.

Alternatively CDP traces are called CMP traces since those traces have common mid point between shot and receiver points. Travel time of CDP traces is expressed by

$$T = \sqrt{T_0^2 + \frac{X^2}{V^2}} \quad (1)$$

Where X is offset (distance between shot point and receiver point), V represents seismic wave velocity and T denotes normal time (travel time at offset zero point). Equation (1) shows that travel time of non zero offset trace is delayed by $dT = T - T_0$ if compared with normal time. If dT , which is called as moveout, is compensated for, then seismic trace may become equivalent regarding to offset distance. This correction is called the NMO (normal moveout) correction and it is one of the most important process to improve the quality of the final seismic section, because stacking of correct NMO corrected traces yield a seismic trace with improved S/N ratio.

Reflection seismic profile so called is made by displaying these stacked tracies sequentially and underground geological structure appears on this profile. One of the most remarkable feature of the CDP stacking is that travel time is expressed by the equation (1) with good approximation regardless of the structure.

This means that improvement of S/N ratio by stacking is still valid for curved and/or multilayered structure.

Stacked seismic profile represents a structure but apparent structure on stacked section is not always the same with the actual one. Due to nondirectioned character of receiver, seismic signal upgoing vertically to the surface is not distinguished from nonvertical signal and they are recorded together on a same seismic trace.

For example, the structure shown to the upper right of Fig. III-2-2- will appear as the left on a seismic profile. This could be easily explained in the following way. NMO corrected trace is equivalent to zero-offset trace, as mentioned, and this means that raypath of NMO corrected trace is perpendicular to the reflector. Then seismic trace at B would have three reflection events from B1', B2' and B3' in contrast one reflection event at A and C. The migration process is a method to convert seismic section to real structure just like from the upper left to the upper right in the figure (III-2-2). The lower of the Fig. III-2-2 represents an actual example of this process. Migrated profile is called as time migrated section if vertical axis is time, or depth migrated section if expressed in depth. It should be noted that NMO correction and migration are geometrical correction. The other common process in the data processing sequence is filtering. This is applied to improve the S/N ratio of seismic traces. Deconvolution, bandpass filter, velocity filter etc. belong to this category. For the details of these processing, refer to the articles listed in the references.

2-2-2 Devices for filed recording and data processing

Instruments as listed in Table 2 were used in 1979 seismic survey at MTA.

Table 2 Instruments used for 1979 Seismic Surve.

Vessel	MTA SISMIK-1 (720 GWT)
Energy Source	Bolt AIR GUNS (40, 20, 10 cubic inches)
Compressor	APS-D20B-500 x 2
Receiver	SEC Streamer with 25 m active section
Recorder	TI DFSIV
Navigation System	MAGNA VOX M x 702/HP satellite navigation system + KRUPP-ATLAS DLOG-12 Doppler Sonar
Computer	TIMAP 980B
Software	MATE-500

Fig. III-2-3 shows the data processing system used for reprocessing at JAPEX.

2-2-3 Seismic Lines.

In the 1979 survey, MTA recorded three high resolution lines and two more normal seismic lines (Kavukçu, 1979, Fig. III-2-4). They are summarized in Table 3.

Table 3 Statistics of Survey Lines

Line	Shot Point	SP Interval	Line Length	Shooting Direction
T1-AB12.5	73-555	12.5 m	7.5 km	NE-SW
T2-AB12.5	0-606	12.5 m	8 km	E-W
T3-AB12.5	1-566	12.5 m	7.5 km	SW-NE
T1-AB25	2-291	25 m	8 km	NE-SW
T2-AB25	13-319	25 m	8 km	E-W

Originally the object of the reprocessing was only high resolution lines. However, due to the difficulty in velocity analysis, longer cable data (normal seismic lines) were also processed to get more reliable velocity information. Line T1-AB12.5 approaches to Kozlu coal field from the approximately 5 km north point of Zonguldak, T2-AB12.5 is a E-W line running from 1.5 km point offshore Zonguldak and crosses seaward extension of the trend of Kozlu coal field. T3-AB12.5 is a nearly parallel line to the shore and north-eastern end lies just offshore Kozlu. Starting point or ending point of each line were located as close as possible to the shore. T1-AB25 is running between T1-AB12.5 and shore line, and the location of the T2-AB25 is the almost same with T2-AB12.5. In the course of data process this time, the portions listed in Table 4 were used after the data quality inquiry.

Table 4 Range of Process

Line	SP Number	Field Rec. No.	Dmuxed Rec. No.
T1-AB12.5	73-555	41-513	1-474
T2-AB12.5	0-606	1-602	1-602
T3-AB12.5	1-554	1-549	1-549
T1-AB25	2-291	1-290	1-290
T2-AB25	-13-319	1-333	1-333

2-3 Field Recording Parameters

Essentially shooting and recording was based on normal reflection seismic survey method. However short cable of 24 channel 600 meter streamer, 1 msec sample interval, small size air gun were utilized to get high resolution data. They are summarized in Table 5.

Table 5 Field Recording Parameters

Survey Lines Parameters	T1-AB12.5 T2-AB12.5 T3-AB12.5	T1-AB25 T2-AB25
No. of Air Gun	3	7
Total Air Gun Volume	70 cubic inch	1685 cubic inch
Air Gun Depth	6 m	15 m
Pressure	1750 PSI	1750
Shot Interval	12.5 m	25
Receiver Group Interval	25 m	25
No. of Channel	24 ch	48
Cable Length	600 m	1200 m
Cable Depth	10 – 15 m	10 – 15 m
Minimum Offset	130 m	150 m
Maximum Offset	705 m	1325 m
CDP Interval	12.5 m	12.5 m
No. of Stack	24	24
Sample Interval	1 ms	2 ms
Record Length	3 sec	4 sec
Low Cut Filter	8/36 Hz/db/oct	8/36 Hz/db/oct
High Cut Filter	248 Hz	124 Hz
Tape Format	SEGB	SEGB
Packing Density	1600 BPI	800 BPI
Constant Gain	24 db	24 db
Gain Control	I.F.P.	I.F.P.

Geometrical relationship between shot and receiver positions is schematically shown in Fig. III-2-5.

2-4 Data Processing

Fig. III-2-6 illustrates the processing sequence. Individual process is not always the same as the originally proposed one for the reprocess. Some of the original are changed according to the data quality or characteristics. In the following, each step of the process will be described together with its result.

Demultiplex

Field recorded data which is multiplexed (channel sequential data) is demultiplexed (converted to trace sequential data) with field recording gain removal. Data edit including omission of bad trace is done at this stage. Recording quality was good enough and no skew and/or parity error were found during the Demultiplex. However, more attention should be paid in order to avoid lack of data and high amplitude noise.

Near Trace Section Display

Near trace seismic sections are displayed (Fig. III-2-7, III-2-8, III-2-9) after the application of digital AAC (Automatic Amplitude Control) of 600 msec window for QC purpose. Although repeated coherent signals on the near trace section may suggest simple water bottom reverberation, they are multiples of reflected refraction and/or refracted reflection as inferred from Fig. III-1-14. This sort of multiple is characterized by its constant slope linear travel time curve regardless of the order of multiples.

One hundred percent record display

All of the shot records were played back for refraction analysis. No gain control was applied before this display since first arrival of refracted wave was so distinct after the gain removal. It was certified through this display that most of primary reflections were masked by strong refraction and its multiples throughout the whole lines. For the reason of this feature, some of frequency analysis, gain recovery and deconvolution tests were carried out after the CDP sorting.

Amplitude Analysis, Gain Recovery Test and Deconvolution Test

1979 seismic data is characterized by impulsive noises as well as the strong refraction multiples (Fig. III-2-7). Those may be originated by electrical shock of recording system. The amplitude of this shock was so strong when compared with normal seismic signal that relative amplitude preservation process by TAR (true amplitude recovery) would bring about poor S/N ratio. On the contrary, AAC might reduce relative amplitude of those shock. Considering these situations, the window length of AAC was tested applying deconvolution and bandpass filters (Fig. III-2-10). On the gain removed shot record which are shown at the

left of Fig. III-2-10, spiky noise is contaminated at about 2.4 second of the trace 24. It is obvious from the figure that smaller AAC window is more effective to suppress the noise. Regarding to the refraction multiple, on the other hand, longer window AAC is more favorable to reject refraction multiples by deconvolution. Thus, the length of AAC window act in opposite way against noise suppression and elimination of refraction multiples. It was decided after preliminary velocity analysis to apply 150 msec AAC for gain recovery because refraction and its multiples could also be attenuated by selecting appropriate stacking velocity. These tests indicate that, in the possible future seismic survey in offshore Zonguldak area, sufficient quality control to keep low noise level is significantly important from the viewpoint of deconvolution effect and multiple suppression.

Deconvolved records are checked by autocorrelograms as in Fig. III-2-11, III-2-12 and III-2-13 on which zero lag autocorrelation is shifted by 200 msec for display purpose. Autocorrelogram after the application of deconvolution of 2000 msec design window, 300 msec operator and 1 msec prediction distance shows that predictable multiples are completely eliminated. In the gain recovery test, 8-80 Hz bandpass filter was applied after the deconvolution. It will be shown later that this filter band is not inconsistent with effective frequency of seismic records.

CDP Sorting

CDP traces were sorted together according to the shooting and recording logs described on observer's note. Basic CDP multiplicity is 24 and CDP interval was 12.5 m. As stated by MTA, shot point is referred to the location of air gun. Taking this definition and effective shot record into account, CDP number was related to the shot point number in the following way.

- T1-AB12.5 CDP No. = SP No. -43.8 (2)
- T2-AB12.5 CDP No. = SP No. +29.2 (3)
- T3-AB12.5 CDP No. = SP No. +29.2 (4)

Total CDP number of line T1-AB12.5, T2-AB12.5 and T3AB12.5 was 505, 630 and 577 respectively. On the most of figures in this report, if not notified, CDP number is being used as a reference. In such occasions, conversion from CDP number to SP number may be made by relationships (2), (3) and (4).

Gain Recovery and Deconvolution

Gain recovery and deconvolution processes were executed after CDP soting. The parameters were 150 msec window for AAC, 2000 msec as design window and 300 msec operator for

whitening deconvolution.

Filter Test before Stack

In addition to the existence of refraction and its multiples, primary reflection is very poor on the seismic records of Zonguldak offshore area as previous reports mentioned. On account of this features, dominant frequencies on the seismic record were tested before stack.

Fig. III-2-14 shows the results of the analysis. Every 10th CDP between 210 and 260 of Line T2-AB12.5 were tested and displayed after trace equalization.

(1) represents original CDP and (2) shows post AAC data. Refraction multiples which have become evident by AAC are attenuated by deconvolution as is shown by (3). Several kinds of bandpass filters are applied to deconvolved records and the results are shown from (4) to (10). It is evident from the figure that higher frequency does not contain considerable information. Namely higher frequency component seems to be representing those events travelled in the water such as direct wave and side reflection. Especially no primary event appears to be represented by higher frequencies for the deeper portion of the section. Same kind of test was performed on CDP 431-435 of line T1-AB25 which were recorded with longer streamer cable (1200 m). The result shown in Fig. III-2-15 exhibits same tendency with previous one (Fig. III-2-14). But higher frequency component is much less important here.

Namely as is shown in (6), frequency components between 30 and 200 Hz indicate no significant coherent event except the portion of first reflection arrival. On the other hand, filtered record with 0-30 Hz frequency band shows remarkably correlated events between traces. Particularly better correlation is clearly shown by the deeper events below two seconds.

So long as frequency is concerned, therefore, it is concluded that 2 msec sampling survey would give the same results with 1 msec survey, because antialiasing filter of conventional 2 msec survey is still around 128 Hz. This does not mean, however, that 1 msec survey is meaningless in this area. This matter will be discussed in 2-6 of this section.

Resample

Under these circumstances, whole data were resampled at 2 msec interval after CDP sorting, AAC and deconvolution before stack. No filter was applied at this stage because recording high cut filter, 248 Hz, was lower than 250 Hz which was the theoretical Niquist frequency

of 2 msec sampling. Actually, higher frequency component than 250 Hz was below -40 db on original near trace as can be seen in Figs. III-1-17a, 17b and 17c.

Velocity analysis

Basic velocity analysis was carried out at every 500 m depth point by constant velocity stack (CVSK) method using 18 velocities and 12 CDP ensemble data. The advantage of this method is, by the use of plural CDP, the characteristics of coherent event can be also shown on the section. For example diffracted events are generally distinguishable from others by their steep slope occurrence. Thus CVSK method is essentially different from other one CDP-based velocity analysis such as constant velocity scan (CVSCAN) or constant velocity gather (CVGATHER). As has been mentioned, however, special geological condition in Zonguldak area make it difficult to derive reliable optimum stacking velocity only from CVSK analysis. Major reason of this difficulty is the limitation of assumed velocity numbers. 18 velocities assumed here for CVSK may be insufficient under the existence of severe refraction multiples. However, it supposed to be time consuming and still deceivable to simply make the number of CVSK velocity larger. After the consideration of situations, it was decided to do additional velocity analyses by CVSCAN and CVGATHER methods.

Not only short cable (600 m) but also long cable (1200 m) data, Line T1-AB25 and T2-AB25, were utilized for the analysis. Furthermore, stacking test was performed assuming several varying velocity functions. For the details of this stacking test, discussion is also made in section IV-1.

[CVSK VELOCITY Analysis]

According to MTA, seismic wave (P wave) velocity of water in Zonguldak area was 1450 m/s. Water depth along the seismic lines is around 100 m except the western end of T2-AB12.5 and T2-AB25. In fact CVSK result shows strong events corresponding to the water bottom when 1450 m/s is assumed (Fig. III-2-18). CVSK also shows coherent signals for the deeper portion of the section. Most of them have low velocity such as 1500-3000 m/s. But these low velocities are unlikely when we consider the existence of high velocity carbonate layer just beneath the water bottom.

As has been indicated (Fig. III-2-14) by refracted events, the velocity of this layer is around 4000 m/s and laboratory measurement of sonic velocity of carbonaceous rocks, which are overlying Carboniferous coal bearing sediment, also shows sonic velocity of several thousands meters per second (Hosono et al, 1970). Taking account of this fact and that significant velocity inversion is improbable, RMS velocity at 0.5 sec depth would be about

3700 m/s. Much higher velocity is expected for deeper portion. Therefore lower velocities shown on velocity diagram (CVSK section etc.) are inconsistent with geological evidences.

In contrast to those low velocity events, some higher velocity events can be recognized on CVSK section. Although most of them are intermittent in occurrence and some are corresponding to refraction and its multiples, one possible velocity function would be determined as solid line in Fig. III-2-18. However correlation of these high velocity events with reflection type travel time curves is generally not definite as can be seen on CVSCAN and CVGATHER sections.

[CVSCAN and CVGATHER Velocity Analysis]

Fig. III-2-19 and Fig. III-2-20 are examples of CVSCAN and CVGATHER velocity analysis respectively. As 70 velocities are used for both analyses, in contrast to the 18 velocities for CVSK, details of velocity spectra is perceptible. In order to assure the analysis, long cable (1200 m) data were used for CVSCAN and CVGATHER. It is obvious from both figures that an event of 3000 m stacking velocity at the depth of sea bottom is corresponding to primary refraction. A series of reflected refraction or refracted reflection shows systematically decreasing velocities from 3000 m in proportion to the order of multiples. In addition to this refraction and its multiples, lower velocity events which appears on CVSK section are also common to all CVSCAN and CVGATHER data.

Primary reflection events are also identified but their occurrence is not so frequent as refraction and its multiples. An event indicated by an arrow in Fig. III-2-21 possibly corresponds to a primary reflection. This event gives 5200 m/s as stacking velocity.

[Velocity Model]

In summarizing the velocity analyses, it was found that definite RMS velocity functions, along time and space, could be hardly determined since the occurrence of primary reflections were limited comparing to the other low velocity events and refraction multiples. Consequently several velocity functions were assumed and NMO correction and stacking were performed using these velocities. Fig. III-2-22 shows the results of this test in which CDP ensemble from 210 to 260 of line T2-AB12.5 were used. Stacking velocity functions assumed here are shown in Fig. III-2-23. L-velocity is very close to a function which is derived from velocity analysis when lower velocity events are selected. T velocity model involves velocity inversion as laboratory measurement of sonic velocity of Carboniferous sediment from Kozlu coal field shows lower velocity than overlying Cretaceous carbonate rock. (Hosono et al., 1970). VELFIL + T-velocity stack section is derived using T-velocity

but velocity filter to reject refraction has been applied before CDP sorting. K-velocity is derived assuming constant velocity of 4000 m/s through the whole layer below the sea bottom. H-velocity is consistent with the average velocity of all possible reflections. HO-velocity function was determined picking up highest possible reflections on velocity analysis profiles. This function is consistent with some high velocity rocks of which sonic velocity was measured by Hosono et al., (1970).

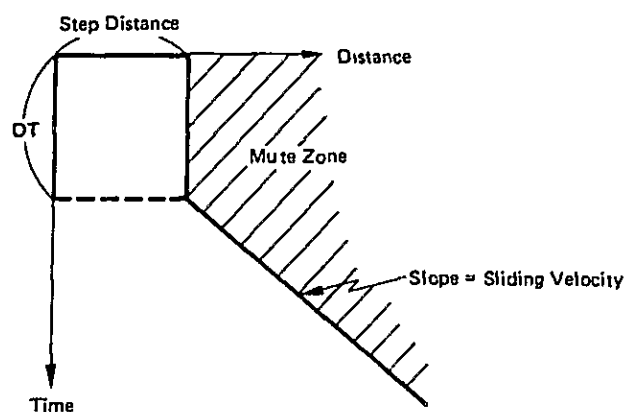
Velocity function has been smoothed in any case of Fig. III-II-22 to avoid rapid velocity change below the sea bottom. On the L-velocity stack section, significant refraction and its multiples masks the shallower structure, from zero to one second. On the other hand, other five cases show very similar results. Namely, no strong refraction effect appears any more.

In consequence, K-velocity is assumed to get stacked sections. In case of line T1-AB12.5 and T3-AB12.5 one velocity function is used for stacking, but space variant velocity function depending on the water depth is applied to line T2-AB12.5.

The velocity functions determined by MTA for the conventional data process were found to be very similar to L-velocity.

NMO Correction and Muting Test

In order to determine optimum mute parameter, several mute parameters were tested. The set of mute parameter was defined in the following way, and some possible sets were selected referring to NMO corrected CDP data.



The main purpose of muting here is to reduce the influence of refractions and direct wave on the stacked section. Stacked profiles after the application of various muting are shown in Fig. III-2-24. In the figure nearest 12 trace stack (NEAR TRACE STACK) and farthest 12 trace stack (FAR TRACE STACK) sections are also shown. Furthermore high frequency

stack section (30-200 Hz) and Low frequency stack section (0-30 Hz) are shown in Fig. III-2-24 to investigate the filtering effect on stacking. The same result as mentioned in filter test before stack is again evident. That is to say, higher frequency gives only poor geological informations.

As a result of this test, a set of mute parameters of 300 m as step distance, 200 ms as DT and 1340 m/s as sliding velocity is selected.

NMO Correction, Muting and Stack

Due to rapid increase of stacking velocity below the sea bottom, automatic mute zone which is determined by the degree of wave stretching was found to be fairly big. On account of this, stretch factor (defined as dT (after NMO)/ dT (before NMO)) of 3.5 was specified at the time of NMO correction. Muting taper was 50 msec and maximum number of fold was 2400%.

Deconvolution Test and Deconvolution

In Figs. III-2-25 and III-2-26 the results of deconvolution test is illustrated. Fig. III-2-26 shows the same deconvolution effect with Fig. III-2-25, but post-decon filter of 8-70 Hz is applied. Concerning to shallow structure just below the sea bottom, deconvolution changes the appearance of the section by eliminating predictive events. Deeper structure below 2.1 sec becomes also clearly visible after the post stack deconvolution.

The quality of the section is changing depending on the depth, from shallower to low frequency deeper portion. Strictly speaking, therefore, time variant deconvolution may be more adequate. Nevertheless, non time variant deconvolution (2000 msec as design window, 2 msec as predictive distance and 200 msec as operator length) was finally selected because of the short record length and insufficient S/N ratio.

Filter Test and Filtering

Post stack filtering test is shown in Fig. III-2-27. As is described in the section of filter test before stack, it is obvious that higher frequency does not include significant information. However in order to avoid making the sections unnatural, time variant filter of 300 msec operator is used. Bandpass frequency is 5-70 Hz, 5-60 Hz and 5-50 Hz, from the shallower to the deeper of the section. It should be noted that lower frequency than field low cut filter is still contained due to finite slope of the filter (see Figs. III-2-17a, b, c.).

Datum correction

Datum correction of 12 msec which is equivalent to the combined effect of gun depth (6 m)

and streamer cable depth (10-15 m) was carried out. Datum correction for longer streamer cable data (T1-AB25 and T2-AB25) was 18 msec since gun depth was 15 m.

Time Migration and Depth Migration

Average velocity was utilized for the both migration. Migration process was made in F-K domain (Stolt 1978). The structure shown by T3-AB12.5 is almost flat and no significant migration effect was obtained on time migrated sections. Migration process collapsed diffractions for the western part of line T2-AB12.5, especially just below the sea bottom. T1-AB12.5 section shows also migrated events. But it appears that migration effect is also reduced due to rapid average velocity increase along the depth axis.

Wavelet Processing Test

Experimental wavelet process, or wavelet deconvolution is performed to get high resolution profile attenuating undesirable later phase. Although total system response including source signature and response of recording system etc. is required for this process, no source signature is available nor extraction of wavelet from sea bottom reflection is not practical from 1979 seismic data.

Accordingly wavelet process test to remove only DFS-IV impulse response is carried out. This method is reasonable and sometimes effective, since nonminimum phase character arises mainly from recorder response in case of air gun source. The impulse response of DFS-IV, when 8/36-248 Hz recording filter is used, is shown in Fig. III-2-28. This response is not minimum phase and it can not be converted to pulse by deconvolution. But if the response is once converted to minimum phase as (2) of Fig. III-2-28, pulse compression by deconvolution gives much better result ((3) of Fig. III-2-28). In Fig. III-2-28, time zero is shifted by 50 msec for the sake of display.

Equivalent process of seismic record should yield later phase free section in the same manner. Fig. III-2-29 shows an example of wavelet process application to selected CDP data of T2-AB12.5. CDP ensemble denoted by (1) are original data and (2) are that wavelet processed (Minimum phase conversion plus deconvolution). (3) shows gain recovered data after the processing. Stacked section of wavelet processed data is shown in Fig. III-2-30. (1), (2) and (3) represent stacked, deconvolved and filtered sections respectively. Comparing to conventionally processed profile, later phase is eliminated but remarkable improvement is not recognized. This may be due to partial wavelet process in which source signature and other responses are ignored. Recording or extraction of practical wavelet is required in the future seismic survey.

2-5 Results of the process

Processed seismic profiles are attached to this report as Enclosure No. 6-14. Long cable (1200 m) seismic profiles are also enclosed for convenience (Enclosure 15-17).

They are summarized in the Table 6 as follows:

Table 6 List of Stacked Sections

Line	Stacked Section	Migrated Time Section	Migrated Depth Section
T1-AB12.5	Encl. 6	Encl. 9	Encl. 12
T2-AB12.5	Encl. 7	Encl. 10	Encl. 13
T3-AB12.5	Encl. 8	Encl. 11	Encl. 14
T1-AB25	Encl. 15, 16	—	—
T2-AB25	Encl. 17	—	—

Seismic sections obtained by the reprocessing this time are completely different from previous sections processed at MTA. The main reason of this is the difference in stacking velocity. The use of low velocity function such as L-velocity defined in this report will yield many coherent events but most of them are relating with refraction, refraction multiples and side reflections. MTA sections have been processed with similar low velocity functions. On the other hand, velocity function used for present reprocessing is consistent with other geological evidences. In addition to the use of high velocity, longer operator deconvolution might also contribute to attenuate the multiples of refraction.

2-6 Discussion

Several facts have been clarified through present work of reprocessing concerning to what must be considered for future seismic survey in offshore Zonguldak area. Before the discussion of survey method itself, the influence of special geological condition in the area should be mentioned. As has been mentioned repeatedly, the characteristic feature on the seismic section in this area is the existence of reflected refraction and/or refracted reflections. These events are different from simple water bottom reflection multiple in the apparent velocity and travelttime curve. Their travel time curve is linear and if their travelttime curve is deemed as hyperbolic, resultant apparent velocity is much higher than the velocity in water. And it would be very close to primary reflection velocity, though travelttime curve of reflection is hyperbolic. Therefore, it might be very difficult to distinguish primary reflections from other undesirable events by stacking velocity only.

This will be the main subject to be solved in the future survey.

Under these conditions, more attention should be paid on streamer cable length and offset. This is the first point to be suggested. In case of reflection seismic survey, it is one of the most fundamental matter to select favorable offset distances. Appearance of reflection, refraction, direct wave and ground roll (Low velocity noise is sometimes recorded even in offshore seismic survey) changes depending on the source-receiver distance, and undesirable event are generally avoidable by adopting proper offset. Since no this sort of test has been reported in offshore Zonguldak so far, it is inevitable to perform so called noise test to investigate the characteristics of various waves. Indeed this test can be performed without requiring any additional equipments because MTA has 3600 m long cable with 75 m active section as well as 25 m active section cable. After accomplishing this test, favorable offset may be derived.

Secondly, continuous survey from deep offshore to shallow offshore may be valuable to study the appearance of primary reflections. As has been pointed out, second characteristic feature of the Zonguldak area is the limited occurrence of primary reflections. The combined effect of strong refraction multiples and poor reflection events makes it difficult to process and interpret seismic data. Under this situation, investigation of near shore seismic data referring adjacent seismic profile in which refraction is not of significance may be valuable.

Thirdly, data acquisition method as well as the streamer cable length should be studied again. For example plane wave travelling downward vertically will give seismic record which are not affected by refraction and its multiples. So, the use of long air gun array instead of conventional array might provide refraction free seismic section or at least attenuated refraction. Air gun array must be spread over 200-300 m for this purpose and this test requires the change of air gun array. However, its possible to simulate such long air gun array provided that reciprocity of raypass can be assumed. Here one simulation is performed using 1979 seismic data. The shot point and receiver point are assumed mutually changeable in the test and stack of fine traces of common shot data is done. The left of Fig. III-2-31 is a 100% CDP record and plane wave simulated CDP is on the right. It is obvious that the amplitude of refraction and multiple is attenuated. In Fig. III-2-32, stack section of plane wave simulated data is compared to conventionally processed profile. Unfortunately the difference between those two sections is minor but combination of proper offset will bring better result. It should be noted that coherent events after plane wave simulation distribute

mostly on small offset traces. This may suggest that short cable is advantageous so far as primary reflection is concerned. Anyhow Figs. III-2-31 and III-2-32 show only experimental simulation and field test is advisable.

Fourthly, the method of high resolution survey may require further test. In 1979 survey small volume air gun array (totally 70 cubic inch) was used with 25 m active section streamer cable in order to detect supposed relatively thin coal bearing Carboniferous layers below high velocity Cretaceous carbonate rocks. The sampling rate was 1 msec for this purpose. However frequency analysis performed during the present process shows no important geological information is provided by high frequency component. This means either high frequency information is masked by strong low frequency component or geological structure of Zonguldak area does not respond to higher frequency. Judging from experiments reported from other fields, actual reason of poor high frequency information may be due to the former situation. The most important recording parameter in such a case is low cut frequency. Many high frequency seismic survey tell us that good high resolution seismic profile is not obtained unless high low cut filter is used. Generally low cut filter of about several tens hertz or more is used in successful high resolution surveys. Therefore, low cut filter test at the time of recording is necessary in future high resolution seismic survey. As a natural result, penetration of seismic energy will decrease if high frequency component is utilized. Accordingly other attentions should be paid if the target depth is fairly big. One method is to use bigger energy source.

The last one which should be pointed out for future work is relating to data process. Deconvolution operator must be long enough to attenuate refraction multiples. If record quality is fairly good, adaptive application of deconvolution will be useful. Concerning to stacking velocity, geological conditions should be taken into account and anomalously low velocity event must be ignored. This is of significance to keep seismic sections away from side reflection. Moreover, velocity filter or F-K filter should be carefully applied (if application is necessary) since reflection event would have very similar slope with refraction multiples, especially on far offset traces.

3. VELOCITY ANALYSIS BY SEISMIC REFRACTION METHOD

3-1 Purpose

The purpose of the velocity analysis by refraction method using the monitor records acquired in the reflection seismic survey in the offshore Zonguldak coal field is to obtain a knowledge on the relationship between the obtained seismic velocity and the corresponding lithology.

3-2 Principle of Seismic Refraction Method

There are several types of the seismic waves, such as a primary wave (longitudinal wave), a secondary wave (transverse wave) and a surface wave. The velocities of them are fundamentally related to the various physical properties namely Yong Modulous, Poisson's Ratio and density of the medium in which seismic wave propagates. In the refraction method, only first arrivals on the record, which are evidences of the fastest travelling wave (primary wave), are concerned. The seismic wave initiated by an energy source spreads out in the medium and it would be picked up by the geophone (or hydrophone in water) as the wave forms having the characteristic frequency and amplitude. The original wave is generally deformed by the effect of absorption, reflection, refraction and diffraction during travelling in the complex underground media. The refraction may take place at the boundary plane between the two different sediments where the velocity discontinuity occurs. By calculating time-distance relations, the velocity of each layer and the depth of boundary can be determined. The above mentioned principle is commonly applied in the refraction seismic survey to elucidate underground geological feature and physical properties of rocks.

3-3 Procedure of Field Operation

With the data acquisition devices, the devices for field recording and data processing were already explained in the aforementioned Section 2-2-2. And the seismic lines and the field recording parameters employed for this survey were also described in the aforementioned Section 2-2-3 and 2-3, respectively.

3-4 Method of Analysis

Usually, the travel time of P-wave will be read off as a propogating time designated between the shot mark and the first arrival of each P-wave on the seismic monitor record. Then the Time-Distance curve will be made by plotting every travel time for every seismic shot. In this work for the offshore Zonguldak survey, the every obvious first peak indicated immediately after the first break of P-wave is picked up instead of the real one. Because it is not easy to read the first arrival mark of P-wave on the record, and there seems to be no parti-

cular problem due to a quite constant lag between the actual first break of P-wave and the first readable peak. The following assumptions were made in the velocity analysis, especially for the propagation of seismic waves in layers:

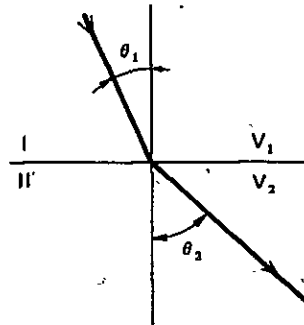
- (a) The seismic wave velocity in the homogeneous medium is constant for every direction.
- (b) The propagation of the seismic wave in the layer is to be followed by the Fermat's principle, i.e. the propagation path of the seismic wave between arbitrary two points will take a minimum travel time.

In other words, the abovementioned assumptions will practically be described as follows:

- 1) The propagation path of the seismic wave in the same velocity layer is to be straight.
- 2) The seismic wave is to be reflected at the boundary between the different velocity layers and the angle of incidence is equal to that of reflection.
- 3) The seismic wave is to be refracted at the boundary between the different velocity layers according to the Law of Refractions which is identical with the term in optics known as Snell's Law.

To recapitulate the Law of Refractions,

$$\frac{\sin\theta_1}{\sin\theta_2} = \frac{V_1}{V_2}$$



θ_1 : Angle of Incidence

θ_2 : Angle of Refraction

- 4) Under the above condition, the propagation path of the seismic wave is reversible and the travel time (T) on the path is the same for the both ways.

$$T_{asrb} = T_{brsa}$$

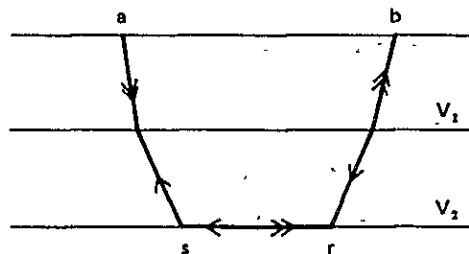


Fig. III-3-1 shows an example of the seismic record which was used for the analysis to pick up the first arrival marks. Observing the first arrivals on each trace of seismic record, a one way time-distance curve can be obtained. But it is evident that, we can not separate the

effect caused by dip of layers and velocity of them. (from a simple seismic profile and corresponding T-D curve) In other words, the velocity of second layer obtained from the single T-D curve is apparent one, not the true velocity. Therefore to carry out the refraction analysis, it is necessary to have the T-D curve of opposite direction started from the corresponding shot point at the opposite side. A pair of T-D curves is to be obtained by utilizing the above mentioned principle 4). The following is the refraction analysis, so-called 'Hagitori Method', used for the two velocity layer's model. In Fig. III-3-2, assuming the thickness $Z(r)$ of the upper medium at the receiver point r which is the arbitrary point in between a and b , the sum of travel time T_{ar} is given by

$$T_{ar} = D_{1,2}(a) + D_{1,2}(r) + a'' \cdot r'' / V_2 \quad \dots \textcircled{1}$$

$$\text{under } D_{1,2}(a) = D_{1,2}(r) = Z \cdot \cos \theta_{1,2} / V_1 \quad \dots \textcircled{2}$$

Where $D_{1,2}(a)$, $D_{1,2}(r)$ is the delay time relating the thickness of the upper velocity layer V_1 at point a and r respectively (in this case, V_1 is the velocity of sea water).

However, in this velocity analysis, the read off mark for the wave arrival time is the

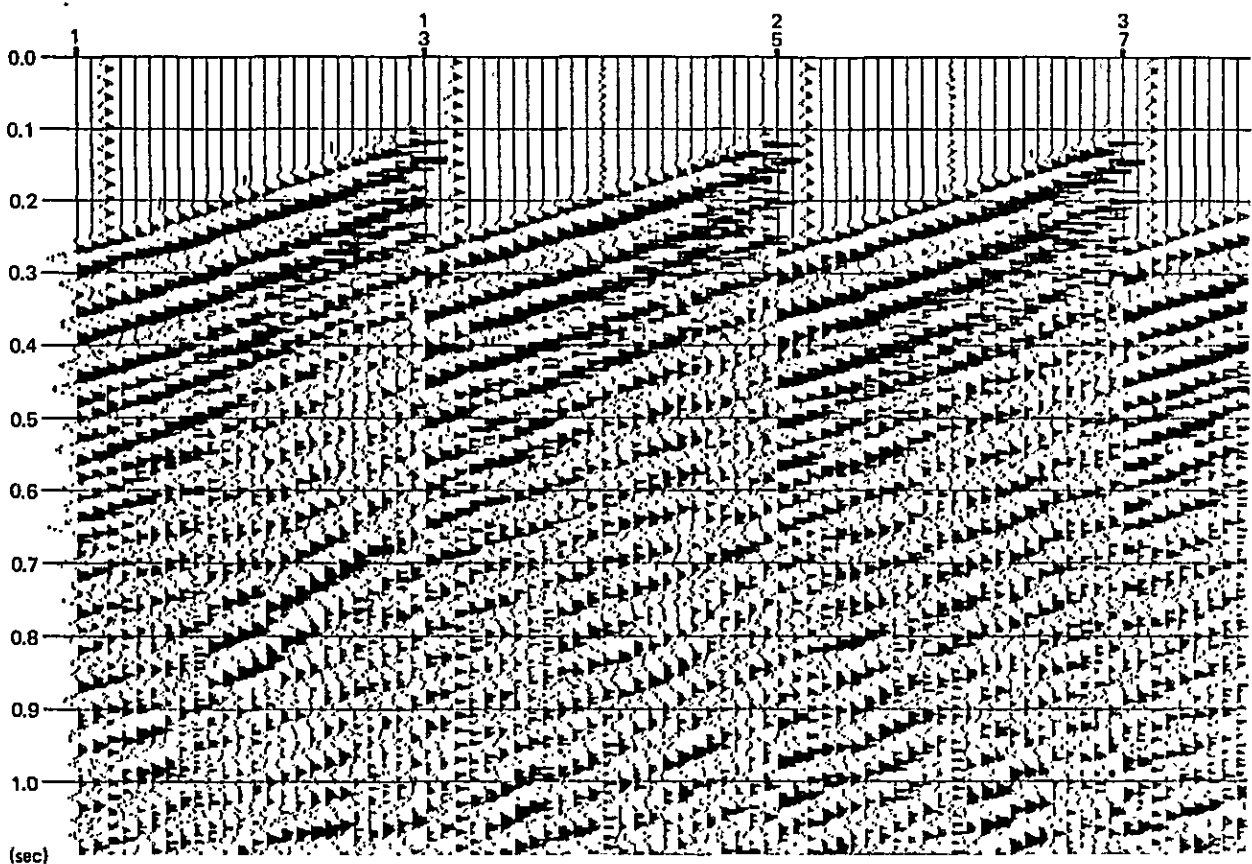


Fig. III-3-1 Examples of seismic records T2-AB (12.5) – Line

ideal one as defined in the aforementioned paragraph. There is a small time lag (ΔT) in the reading, therefore, the equation (1) should be written as

$$\overline{\Pi}_{ar} = D_{1,2}(a) + D_{1,2}(r) + a'' \cdot r''/V_2 + \Delta T_a \quad \dots (3)$$

or
$$\overline{\Pi}_{ab} = D_{1,2}(a) + D_{1,2}(b) + a'' \cdot r''/V_2 + \Delta T_a \quad \dots (4)$$

or
$$\overline{\Pi}_{rb} = D_{1,2}(r) + D_{1,2}(b) + r'' \cdot b''/V_2 + \Delta T_r \quad \dots (5)$$

The artificially inferred curve $\overline{\Pi}_{b-}$ will be drawn by two points marked as a circle on each time line of a and r. These two points are to be determined from the arrival end times $\overline{\Pi}_{ab}$ and $\overline{\Pi}_{rb}$ at location b. Therefore,

$$\overline{\Pi}_{ab} = \overline{\Pi}_{ba} \quad \dots (6)$$

and
$$\overline{\Pi}_{rb} = \overline{\Pi}_{br} \quad \dots (7)$$

Each, ΔT_a and ΔT_r is, herein, to be recognized as a constant value for all the readings.

When the time difference, DT , between observed T-D curve and so called 'Hagitori' T-D curve is assumed as the following relationship:

$$DT = (\overline{\Pi}_{ar} + \overline{\Pi}_{br} - \overline{\Pi}_{ab})/2 \quad \dots (8)$$

This equation can be re-written by employing formulas of (3) - (7), as

$$DT = D_{1,2}(r) + \Delta T_a/2 \quad \dots (9)$$

When T'_{ar} so called 'Hagitori' point, is represented by

$$T'_{ar} = \overline{\Pi}_{ar} - DT \quad \dots (10)$$

then
$$T'_{ar} = \underline{D_{1,2}(a) + \Delta T_a/2} + a'' \cdot r''/V_2 \quad \dots (11)$$

The summation under lined in the equation (11) can be considered as a constant value, therefore, the seismic wave velocity V_2 will be given by measuring the gradient of the obtained time-distance curve. The 'Hagitori' points (T'_{ar}) are plotted in Encl. 18-21 according to the calculation upon equation (11). In each of the graph shown in Encl. 18-21, a solid line connecting 'Hagitori' points shows the 'Hagitori' T-D curve derived from the observed curve and a line which has the reversed slope is made by calculation.

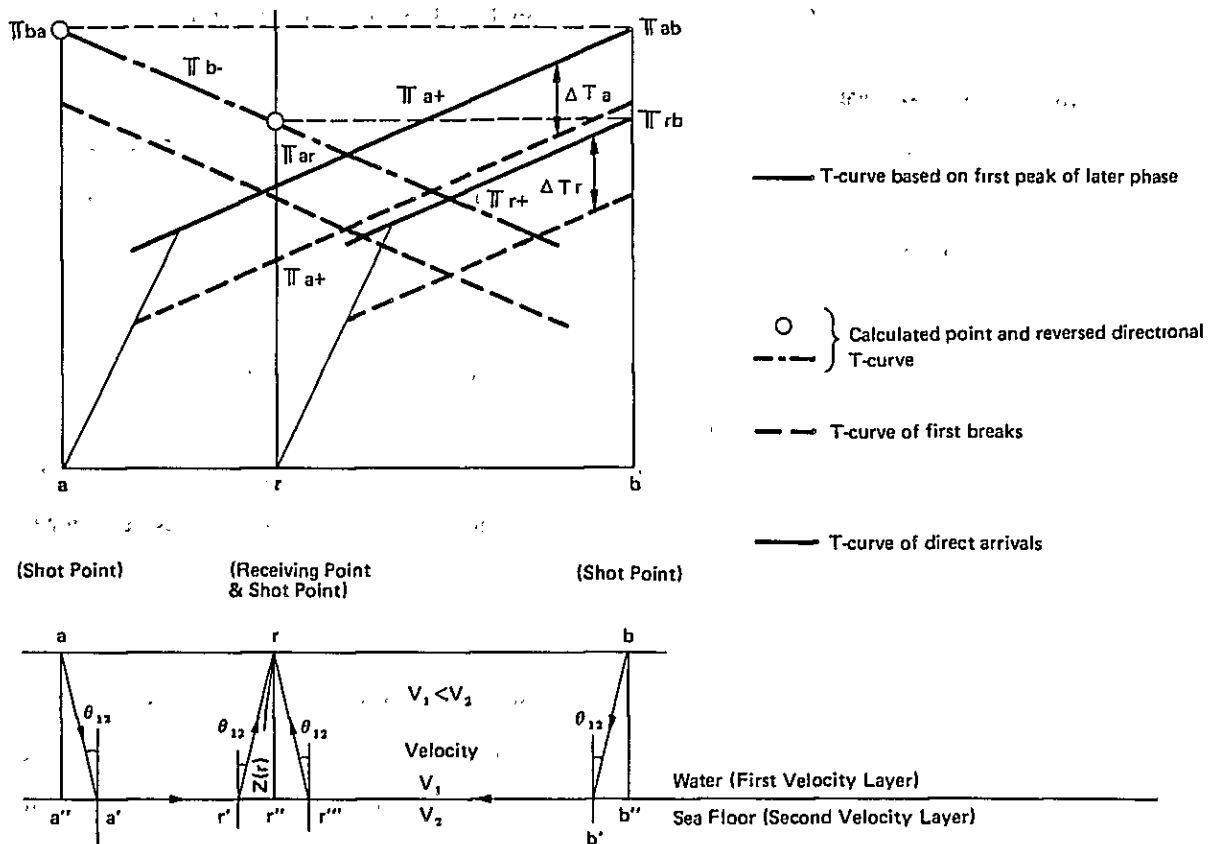


Fig. III-3-2 Explanation of the T-D curve and Velocity Section

Using these pairs of curves, the velocity analysis have been carried out for each seismic line. And the calculated velocities are summarized in Fig. III-3-3.

It is necessary that the time lag error (ΔT_a) must be reduced into a negligible order to obtain a reliable thickness of the second layer (sea floor bed). In another word, if the exact time of the first break could be picked up, it is possible to calculate the actual depth of the refractor. However, it is generally difficult to find the exact arrival time under various conditions. The undesirable factors which may cause to introduce some errors in the reading of the arrival time are:

- (a) on resolution of the recording system,
- (b) on resolution of the display devices,
- (c) on the human made error in the reading of the arrival time. and

(d) on the positioning which may cause the error in horizontal distance determination between the shot point and receiving point.

Owing to these factors, 5 – 10% of error can be included in all computed values.

3-5 Results of the Analysis

Distribution of the calculated velocity along the geophysical survey lines offshore Zonguldak area is shown in Fig. IV-2-2. A corresponding T-D curves are illustrated in attached Encl. 18-21. The results are summarized in the following subparagraphs per survey line.

3-5-1 T₁-AB (12.5 m)

The velocities ranging from 3.9 to 4.0 km/sec are most frequently obtained throughout the line. But comparatively high velocities, more than 4.5 km/sec are partly recognized in the near coast (around SP.480), in the middle (around SP.280) and in the northern end (around SP.70–150) of the line, while a relatively low velocity, about 3.3 km/sec, is recognized around the middle of the line (SP.214–230).

3-5-2 T₁-AB (25 m)

The velocities of 3.6 – 3.9 km/sec are also commonly shown in this line, but the high velocity outstandingly appears at the south end of the line where the limestone is exposed nearby peninsula. Another comparatively high velocity about 4.4 km/sec is obtained around SP.220–235. A relatively low velocity about 3.1 km/sec appears around SP.80–85 in the north-east end.

3-5-3 T₂-AB (12.5 m)

A couple of relatively low velocity zones of 3.0 km/sec is obtained inbetween the T₁-AB (12.5) and T₁-AB(25) lines, and another low velocity of 2.5 km/sec is calculated at the subsurface hollow in the west end. A relatively big lateral change in the velocity distribution was observed on this line though there was no significant high velocity.

3-5-4 T₃-AB (12.5 m)

The very monotonous velocity of 3.8 km/sec is obtained in the southwest half of the line. On the other side, the northeast half is occupied by the various velocity segments. The significant low velocity of 2.8 km/sec is calculated around SP.410, lying within the relatively low velocity zone of 3.2 – 3.5 km/sec. In the northeast end of the line, a comparatively high velocity zone of 4.1 km/sec, appears, of which the extension of the limestone exposures nearby Kozlu could be inferred. A locally low anomaly exists in the above high velocity distribution area as a prolongation of the Karadon fault.

3-6 Considerations

3-6-1 General consideration

The refraction analysis is carried out under the following assumptions.

- a) The influence of the sea bottom topography in the calculation is ignorable, because it is dipping toward the offshore with very small angle of about 2 degrees and the bottom feature is generally very smooth.
- b) In each of the seismic monitor record, two significant first arrivals representing the velocities of the sea water and the underlying medium are observed as a relatively clear break of arrivals.
- c) There are no obvious second breaks on the T-D curves and even on the records acquired by the long cable.
- d) At the west-end of the T₂-AB line, only the direct wave propagation in water has been strongly recorded where the water depth exceeds 150 meters.

Several estimations are made with the above conditions.

- (1) It seems that overlying Tertiary and/or Quaternary sediments seem to exist in some places. In the case, if there are no young sediments, a high velocity arrivals of ± 4.0 km/sec appear immediately after the water. An estimation was made to know the approximate thickness of the recent sediment upon the following assumptions:

- Water depth : 60 meters
- Velocity of water (first layer) : 1.45 km/sec
- Velocity of third layer below the recent sediment : 5.0 km/sec
- If velocity by recent sediment (second layer) is 2.0 km/sec and 2.5 km/sec.

The each thickness of recent sediment based on the two different velocities of them will be 50 meters or 20 meters respectively.

- (2) In order to know the geological structure such as monoclinical, anticlinal or synclinal structures, it is necessary to know a) the velocity of seafloor(V_2) and that of its succeeding layer(V_3) b) the estimated thickness of V_2 layer based on the results of time-distance curve. However, there is no second breaking point in the time-distance curve. Then, two possible cases are to be considered:

- 1) The second layer is very thick. In that case, the following geological model will be estimated under the assumptions, such as:
 - a) Velocity of sea water(V_1) is 1.45 km/sec.
 - b) Velocity of seafloor(V_2) is 4.0 km/sec.
 - c) If the second break occurs at the distance of 1.3 km from the shooting point

(in another word, it is at the end of streamer cable).

d) If the velocity of third layer(V_2) ranges from 4.1 to 4.5 km/sec.

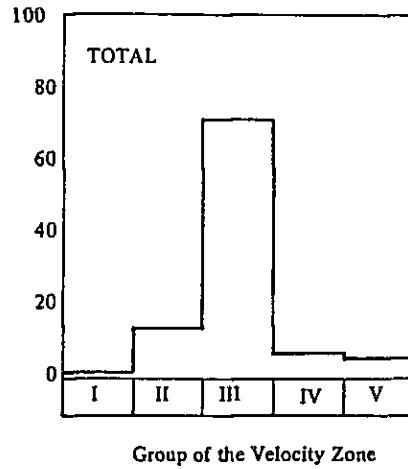
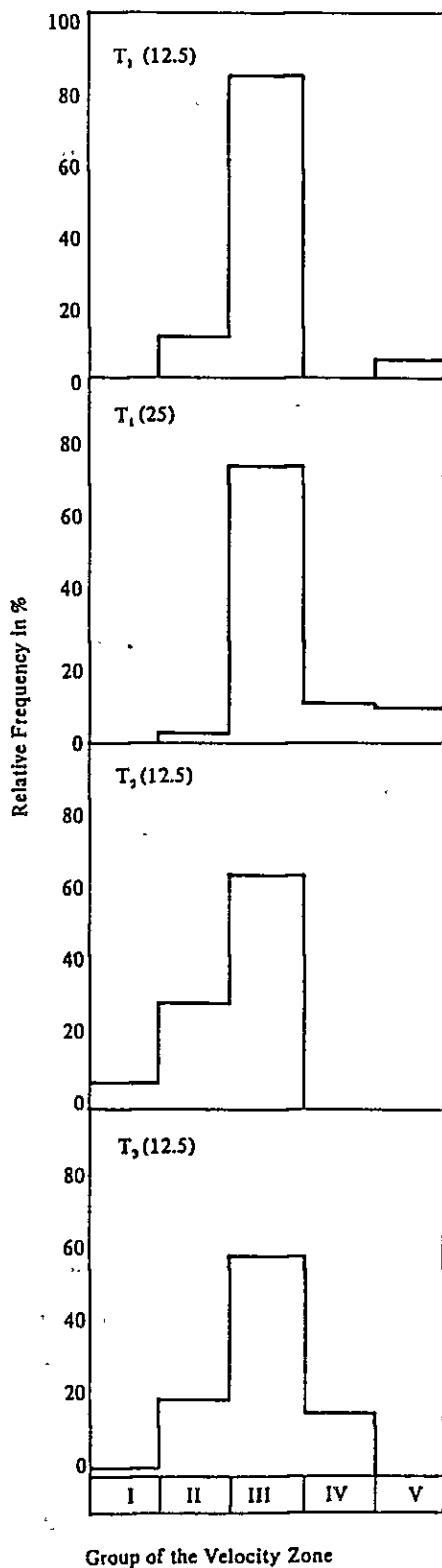
The thickness of the second layer will be in a range between 150 meters and 250 meters.

- 2) If the velocity of second layer is higher than that of third layer, there may be no second breaking point on the time-distance curve regardless the thickness of the second layer. In this case, the velocity of the third layer is probably smaller than 4 km/sec.
- (3) The 200 meters is the maximum applicable water depth for this refraction analysis method with the long spread cable (1,200 meters length), and 100 meters with the short cable (600 meter length).

3-6-2 Results and statistics

Reviewing the velocity distribution map shown in Fig. IV-2-2 and the histogram in Fig. III-3-3, the following observations can be summarized.

- (1) Some characteristic velocities have been obtained in this area, and the full range of the velocity is from 2.5 to 5.6 km/sec.
- (2) Lateral velocity change was most significantly shown on the line T_2 -AB(12.5). On the contrary, velocity variation was very small on the line T_1 -AB(12.5).
- (3) There was no significant velocity change toward the offshore.
- (4) However, several high velocities have been obtained locally nearby the limestone exposures on land and other areas.
- (5) In the Fig. III-3-3, the distinguished velocities range from 3.6 to 4.0 km/sec by which more than 60% over the lines has been occupied.



LEGEND

Group	Velocity (km/sec)
I	$3.0 \leq$
II	3.1 ~ 3.5
III	3.6 ~ 4.0
IV	4.1 ~ 4.5
V	$4.6 \leq$

Fig. III-3-3 Histogram of the Velocity Group obtained by Refraction Analysis (per line & total)

4. PROCESSING OF GRAVITY AND MAGNETIC DATA

4-1 Purpose

The primary purpose of this investigation was to evaluate an adaptability of gravity and magnetic method as a supplementary measures in depicting the basement structure and the distribution of igneous bodies in the area offshore Zonguldak Coal Field. To achieve those, quantitative and qualitative interpretation methods were applied to the all data acquired onland and offshore Zonguldak area. As a total coverage of offshore data was not sufficient enough to analyze the geological features, the interpretation was mainly devoted to onland area and then extended toward offshore area.

4-2 Survey Method

4-2-1 Equipment

Table 7 shows the type of the equipment used for the surveys. This is based on the brochure of M.T.A. (5) and the information from Mr. Kenan Eres and Mr. Sinan Kavkcü, trainees of JICA, 1980.

Table 7 Gravity and Magnetic Equipment

	Offshore	Onland
Gravity Survey	LaCoste & Romberg Air/Sea Gravity meter Model-S	Wordon Gravity meter
Magnetic Survey	Barringer M-123 Recording Magnetometer Sensor: 229 m, deep marine Power: 3A at 24 V	Flux-gate Magnetometer (Air borne Type)

4-2-2 Coverage of gravity and magnetic survey

Offshore gravity, magnetic and seismic data were acquired simultaneously during seismic survey. A total of four traverse lines covering 31.0 kilometers was surveyed. According to 'Technical Cooperation Report' by Mr. Bojo and Mr. Tsu (2), the interval of onland gravity observation points is approximately 500 meters along roads or paths. In the previously made the aeromagnetic survey previously made was carried out under the following conditions. a) the direction of the flight course is N 45 degree W, b) the spacing of lines is at approximately 500 meters and the mean flight height is 150 meters above the ground.

4-3 Data Processing

In general, both the gravitational and magnetic potential fields always involve the regional and residual effects. The fundamental problem is how to separate these effects and interpret

them under the geologic terms. Many different types of method for gravity and magnetic interpretations are developed up to now. For the present interpretation, the following analyses were applied by using computer processing system.

4-3-1 Processing of Gravity data

(1) Residual gravity calculation

This method is based on the Seya's running average method (10) which is a kind of Band-pass filtering procedure. It allows to extract some geologically interesting features by eliminating sharp anomalies of shallow origin (or noise) and very broad band anomalies caused by the geologically regional nature. In this method, grid system is firstly drawn on the Bouguer Anomaly Map with an adequate spacing which is to be approximately the same distance with the depth to be investigated (1 km in this case). Then Bouguer gravity value at every grid points is read off for the preparation of the following formula.

– To extract high frequency component of gravity field.

(Noise or shallow origin)

$$GN(m,n) = g(m,n) - \frac{\sum_{i=m-1}^{m+1} \sum_{j=n-1}^{n+1} g(i,j)}{9} \dots\dots\dots (1)$$

– To extract intermediate frequency component.

(Normal structure)

$$GN(m,n) = \frac{\sum_{i=m-1}^{m+1} \sum_{j=n-1}^{n+1} g(i,j)}{9} - \frac{\sum_{i=m-3}^{m+3} \sum_{j=n-3}^{n+3} g(i,j)}{49} \dots\dots\dots (2)$$

– To extract low frequency component.

(Regional origin)

$$GR(m,n) = \frac{\sum_{i=m-3}^{m+3} \sum_{j=n-3}^{n+3} g(i,j)}{49} - \frac{\sum_{i=m-1}^{m+1} \sum_{j=n-1}^{n+1} g(i,j)}{225} \dots\dots\dots (3)$$

Where $g(i, j)$ is a reading of Bouguer value at the grid point (i, j) . Equation (1), which is a difference in Bouguer gravity between the observed value at the center point and the average of nine readings around the center point, may represent relatively sharp anomalies caused by the shallow geological origin, or the man made errors.

Equation (2), gravity difference between average of nine readings and that of 49 readings around the center point, may represents anomalies with intermediate dimension or "Normal structure" which may be the most probable indicative of geologically

interesting source.

Equation (3) represents very broad anomalies of a regional geological nature.

These calculations are performed for every grid points of onland Bouguer gravity map and three different residual gravity maps are thus obtained. Among these maps, 'Normal structure map' seems to reflect the possible geological structure in this area.

(2) Two-dimensional curve matching method

A curve matching method with two dimensional and infinite horizontal sheets has been occasionally used to analyze the gravity data because of its simplicity in handling. In this method, a gravity effect at a surface point P is calculated assuming a subsurface model which may be composed of several horizontally extended infinite sheets as shown in Fig. III-4-1.

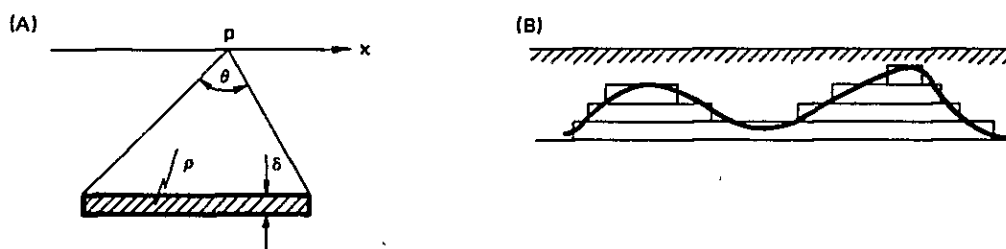


Fig. III-4-1 Two-dimensional Horizontal Plate Model

$$gG(P) = 2 \cdot G \cdot \theta \cdot \rho \cdot \delta$$

where G: Constant universal gravitation

$$(6.67 \times 10^{-8} \text{ dyne} \cdot \text{cm}^2 \cdot \text{g}^{-2})$$

θ : Included angle at P between both end of the sheet (degree)

ρ : density (g/cm^3)

δ : thickness of sheet (km)

If milligal is used as a unit of constant universal gravitation, the above relation is given by

$$gG(P) = 0.2328 \cdot \theta \cdot \rho \cdot \delta$$

A total gravity effect caused by the overall subsurface model at point P is thus calculated by summing up individual effect of each sheet. To obtain a simulated subsurface structure, this calculation is carried out with a considerable interval along X-axis by changing the value of θ , and until the calculated profile is closely fitted to the observed one. In this study, this calculation is tried into two profiles, A-A' and B-B', in

Fig. IV-3-2, and the results are illustrated in the lower profile of each Fig. III-4-3 and Fig. III-4-4.

4-3-2 Analysis of Magnetic data

(1) Qualitative method

The magnetic total intensity map of the onland area shows a relatively good correlation with the distribution of tuff and volcanics of the upper Cretaceous, therefore a qualitative interpretation analysis by using the filtering method was not carried out.

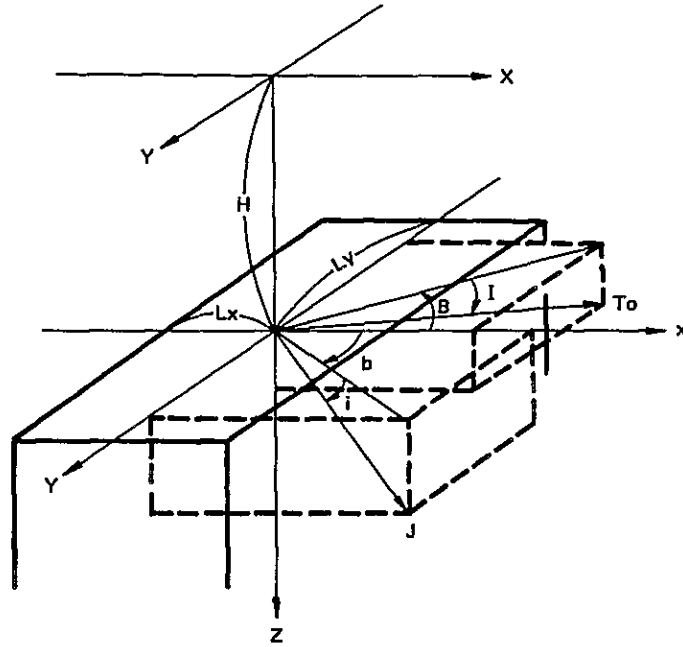
(2) Quantitative method

Tsu's method, which is basically based on the principle of three dimensional prism model, was used as a quantitative method. Assuming the first approximation of a subsurface magnetic body, the calculation was carried out by changing parameters (width and depth) of the prism model until the best fit curve has been obtained. A conversational mode using a Graphic display system combined with big capacity computer is nowadays successfully used for this sort of simulation. The basic formula is given by,

$$\begin{aligned} \Delta T(x, y, H) &= J \cdot G(x, y, H) \\ G(x, y, H) &= \left(\frac{a_{23}}{2}\right) \log\left(\frac{\gamma_0 - a_1}{\gamma_0 + a_1}\right) + \frac{a_{13}}{2} \log\left(\frac{\gamma_0 - \beta_1}{\gamma_0 + \beta_1}\right) - a_{12} \log(\gamma_0 + H) \\ &\quad - IL \tan^{-1}\left(\frac{a_1 \beta_1}{\gamma_0^2 + \gamma_0 H - \beta_1}\right) - mM \tan^{-1}\left(\frac{a_1 \beta_1}{\gamma_0^2 + \gamma_0 H - a_1^2}\right) \\ &\quad + nN \tan^{-1}\left(\frac{a_1 \beta_1}{\gamma_0 H}\right) \left| \frac{a_u}{a_l} \right| \frac{\beta_u}{\beta_l} \end{aligned}$$

Where

$$\begin{aligned} \alpha_1 &= \alpha - x, \beta_1 = \beta - Y \\ \alpha_n &= Lx - x, \alpha_l = -Lx - x, \beta_n = Ly - Y, \beta_l = -Ln - Y \\ \gamma_0 &= (\alpha - x)^2 + (\beta - y)^2 + H^2 \end{aligned}$$



Where

H: Depth to the top of the prism from the plane of observation (x, y)

Lx, Ly: Half width of the prism

\vec{J} : Magnetization vector of the prism

J: Intensity of J

\vec{T}_0 : Vector of the earth's main magnetic field

To: Total intensity of the earth's main magnetic field

l,m,n: Direction cosine of the magnetization vector of \vec{J}

$(l,m,n) = (\cos i \cos b, \cos i \sin b, \sin i)$

L,M,N: Direction cosine of the earth's main field \vec{T}_0

$(L,M,N) = (\cos I \cos B, \cos I \sin B, \sin I)$

i: Angle of inclination of \vec{J}

I: Angle of inclination of \vec{T}_0

b: Angle between the horizontal projection of J and the positive X axis

B: Angle between the horizontal projection of \vec{T}_0 and the positive X axis

Fig. III-4-2 Principle of Magnetic Analysis on Three-dimensional Prism Model

4-4 Discussion for Gravity Result

Gravity analysis was mainly conducted on the basis of Bouguer Gravity map acquired onland area because of the insufficiency of offshore data. Further, the adaptability of this method as a supplementary measure was examined in an attempt to obtain the basic knowledge on the future exploration policy in offshore area.

4-4-1 Bouguer anomaly map

Properly speaking, the same data processing should be applied when the offshore gravity map is expected to combine with onshore one. Since no significant discrepancy was found on the compiled map, the onland Bouguer gravity map was used without applying any correction. In comparison with geological map (1) and compilation map (1), the Bouguer gravity map suggests that:

- 1) In general, the distribution of limestone of the lower Carboniferous and sandy limestone of the Devonian is inconsistent with the shape of the Bouguer gravitational high, which is generally considered to be affected by the high density material.
- 2) A basin structure is existing in the area to the east of Zonguldak, but as far as the Bouguer anomaly map is concerned, there is no significant evidence which is suggesting the existence of this basin at that area. The area of this sedimentary basin is covered by the flank of gravitational high dipping toward the northwest. From this, it can be said that the Bouguer anomaly does not always show the local geological structure in this area due to its complexity. Therefore, the following processing was undertaken in order to emphasize specific frequency component.

4-4-2 Residual gravity map

Aiming to emphasize, shallow, intermediate and deep gravitational information, three kinds of Running average calculation were carried out. Out of which the 'Normal structure map' (intermediate information) computed by equation (2) in page 51 seems to express most clearly the local geological features (Fig. IV-3-2).

- 1) The positive anomalies on this map coincide with the parts of Palaeozoic exposures in some places.
- 2) A gravitational basin is recognized in the area around east of Zonguldak where a sedimental basin of the Carboniferous is recognized.
- 3) Moreover, the map indicates the existence of a fault, which runs at about 20 km south-east of Zonguldak parallel to the coast line, more clearly than Bouguer anomaly map.

The gravity data are not widely collected in the offshore area. However, the abovementioned results may suggest that the further gravity measurement will be recommendable as one of

the feasible geophysical method in the future offshore explorations.

4-4-3 Gravity profiles

The observed residual gravity profiles (upper part of each the figure) are shown in Fig. III-4-3 and Fig. III-4-4, and the final sections of accumulated horizontal sheets computed by the two-dimensional curve matching method are also illustrated (lower part). In this calculation, a density contrast of 0.3 g/cm^3 was assumed on reference to the data presented in the cooperation report by Bojo and Tsu (2).

Profile A-A' : It is obvious that the subsurface model forms an upheaval structure with relatively steep slope at the both ends of the profile. The slope at the south-east side (A' side) of the figure is believed to be an expression of a fault which is already recognized at 20 km southeast of Zonguldak. The slope at the northwest side of the figure is situated nearly 1 km off the coast and this appears to be related to a fault or a discontinuity of high density material.

Profile B-B' : A steep slope of gravity at the northwest side (B' side) also suggests the existence of a fault. The location of B-B' profile is close to the gravity profile (P-12) of the figure-11 in 'Technical cooperation report' (1).

According to the data shown in the report, there is little difference in density between limestones of the Upper Mesozoic and the Lower Palaeozoic. Therefore, to distinguish these limestones by the gravity map will be not easy.

From those, it is anticipated that the high density material is dipping steeply toward the seaward. To know the more detail geological structure, additional offshore data will be required and also the measurement of the density of various rocks distributed in the area will be essential.

4-5 Discussion for Magnetic Result

4-5-1 Total magnetic intensity map

As mentioned before, it was recognized that distribution of tuff and volcanics of the upper Cretaceous seems to coincide with that of the total magnetic intensity. From this, other rocks, regardless of their geological age, appear to have a relatively low magnetic susceptibilities. A tendency of progressive increase in the total magnetic intensity toward the seaward was recognized. This may be due to the regional effect of the earth magnetism. If more detail intensity maps covering more wide range will be acquired by the further offshore exploration in future, I.G.R.F.* correction should be applied to eliminate this regional

Note: *I.G.R.F. – International Geomagnetic Reference Field

gradient effect. However, no regional reduction was made in this study, since a relatively good correlation between magnetic anomaly and geology was recognized.

4-5-2 Profile of Total magnetic intensity

The total magnetic intensity profiles are also illustrated in Fig. III-4-3 and III-4-4 together with gravity profiles. In comparison with gravity data, the magnetic anomaly appears to be found at the gravitational steep slope. On the other hand, as mentioned before, the magnetic anomalies seem to be caused by tuff and/or volcanics of the upper Cretaceous. The details in the relationship between the magnetic and gravity anomalies should be further studied in the future by obtaining additional data. The fact implies that the use of magnetic method in combination with gravity as well as seismic may give a better understanding of these results and make it possible to obtain some knowledge on the structure of the coal bearing strata. In Fig. IV-3-1, the magnetic profiles obtained in this survey are draughted with the gravity contours. At around middle of T2-AB line, a significant pair of magnetic anomalies (positive & negative) is observed which has been already known in the previous survey 1970 (3). On the other hand, there is a magnetic anomaly at the northeast part of T1-AB (12.5) line. Also at the east end of T1-AB (25) line an another small anomaly is observed.

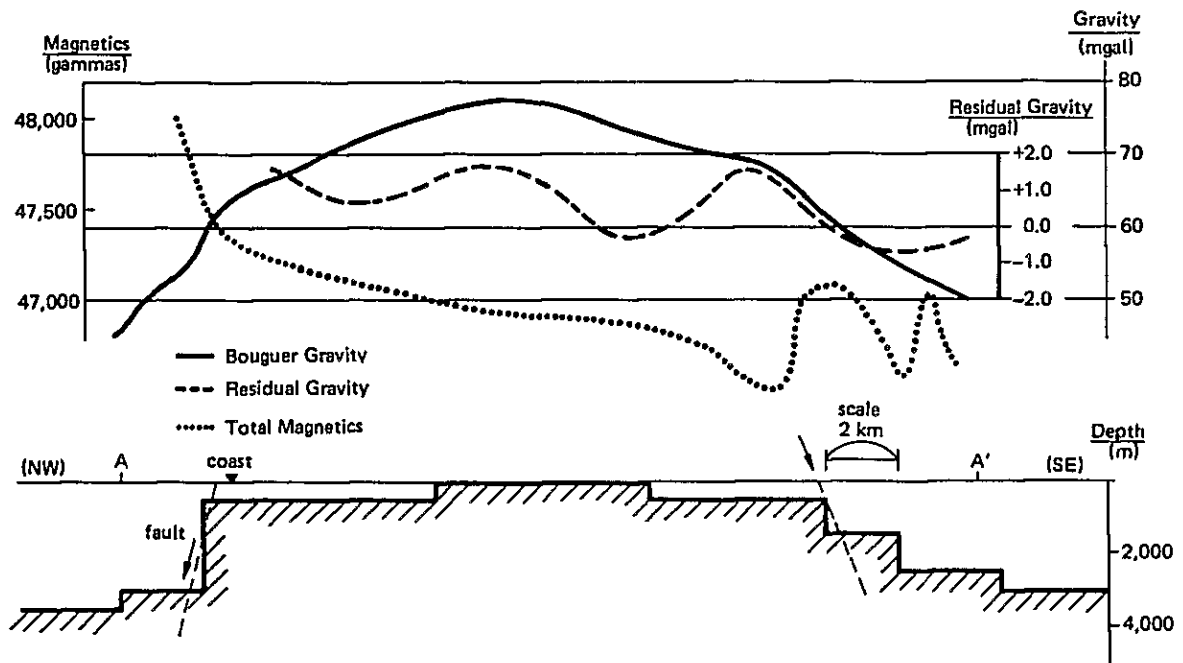


Fig. III-4-3 Gravity/Magnetic Profiles (A-A') and Two-dimensional Interpretation using Gravity

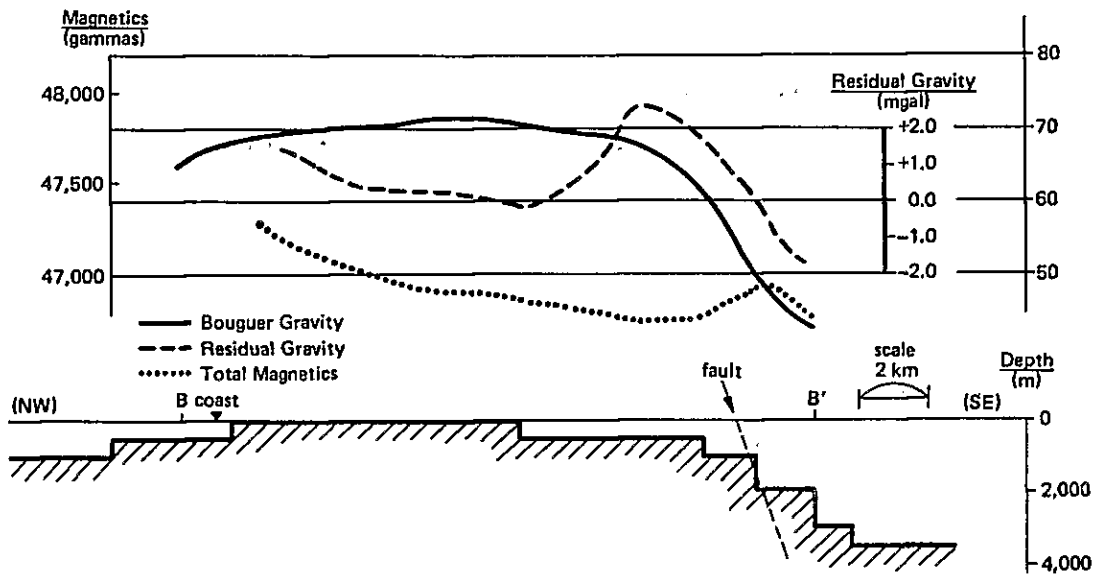


Fig. III-4-4 Gravity/Magnetic Profiles (B-B') and Two-dimensional Interpretation using Gravity Anomaly

4-5-3 Result of three dimensional magnetic interpretation

The necessary condition of three dimensional interpretation is to find a pair of positive and negative anomaly on the total magnetic intensity map. A pair of anomalies around SP.409 on T2-AB (12.5) line was chosen and Tsu's method was applied to this pair. Fig. III-4-5 shows the result of this calculation. In the same manner, the calculation was done on the magnetic body which was found in 1970 survey as illustrated in Fig. III-4-6. Also onshore data were calculated by the same method. The result of this calculation indicates a magnetic body of approximately the same dimension as shown in Fig. III-4-6.

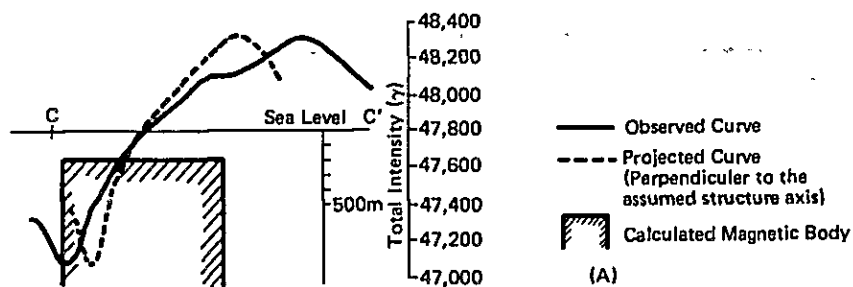


Fig. III-4-5 Quantitative Interpretation using Magnetic Profile

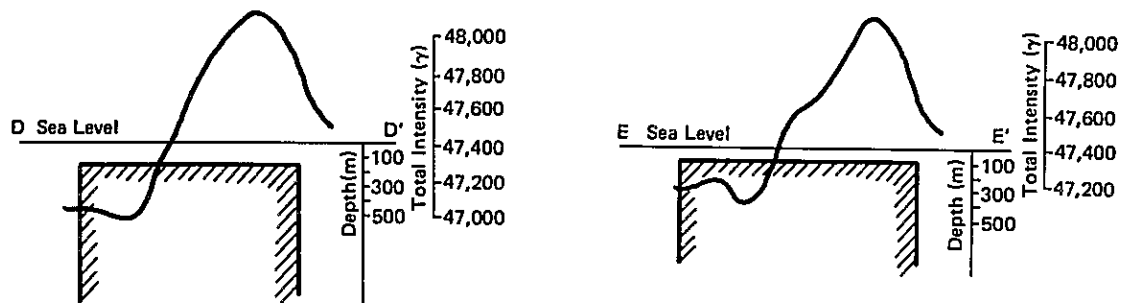


Fig. III-4-6 Quantitative Interpretation using Magnetic Profiles

IV. EXAMINATION OF ACQUIRED RESULTS

Handwritten text, possibly bleed-through from the reverse side of the page. The text is extremely faint and illegible due to low contrast and noise. It appears to be a list or a series of entries, possibly containing names and dates, but the specific content cannot be discerned.

IV. EXAMINATION OF ACQUIRED RESULTS

1. EXAMINATION OF REFLECTION RESULTS

1-1 Examination principle

Relations between basic data acquired by multi-channel recording and some displays are shown on Fig. IV-1-1. Each channel's data collected in field were digitally recorded on magnetic tapes in sequential order of shot family units along the surface named as field shot record. This figure intended to show three dimensional relations among each vertical plane is too mixed up, therefore, to assist easy understanding, plan view relations are shown on Fig. IV-1-2, and it is also shown, for example, on Fig. IV-1-3 that how same reflection events appear on the near trace section, shot record, and CDP family display. There should be common offset section (including far trace section) and common receiving point family (reciprocal to common shot point family), too. Stack section can be treated as different common offset sections after NMO correction of same velocity function piled up on near trace section.

Predominant shallow flat events on seismic section which were thought at first as multiple reflections are now confidently considered to be sea bed multiple refractions (i.e., multiply reflected refraction, after P.N.S. O'Brien, 1957), with addition of some multiple reflections. An example of multiple refraction is clearly shown as straight and repetitive lined up events on Fig. IV-1-4. Meantime, too steeply dipping (too low apparent velocity) events on seismic section which exceed some restriction must not be considered as usual reflections. According to following relations including eqs. (1) and (2), apparent velocity of events can not be lower than medium velocity in which reflection path penetrates. For instance, if some event has apparent velocity of 1.45 km/s, which corresponds to water velocity, or nearly 4 km/s, which corresponds to presumed average rock velocity in this area, these events in the medium of above velocities should show reflection dip of about 90. (Unfortunately such high velocity as 4 km/s must be assumed, according to general considerations about geological age of Carboniferous and Cretaceous rocks, including hard limestone-dolomite facies, and actual measurement results of above rock samples (Hosono et al, 1970) acquired in nearby mining shaft and surface.) These events sometimes may indicate anomalous configuration of seabed (in the case of 1.45 km/s), or fault or reef edge diffraction (in the case of nearly 4 km/s), at sometimes may mean very strong coherent noise remainder incompletely suppressed by data processing. This kind of events was handled with special care. Here, apparent velocity is defined as follows.

$$V_{app.} = 2X/\Delta T \dots\dots\dots (1)$$

Where,

ΔT : time difference between two points on some event.

X : horizontal distance between two points mentioned above on the event.

$X = n \times \Delta X$ (n : number of trace interval, ΔX : depth point interval, 12.5 m on this survey)

if this event is considered as reflection,

$$V_{app.} = V/\sin\theta \dots\dots\dots (2)$$

Where,

V : rock velocity in the case of horizontal sea bed

θ : dip of reflector

Finally writers considered that such steep dip events more than 4 km/s of apparent velocity and shallow event mentioned above are showing no reflection of sufficiently penetrated seismic wave in general.

Normally events of non geological information like described above are eliminated enough by means of stack effects or other kind of filtering processing on final stack section. However, in this survey it is possible to pick up remainings of false reflections rather than true reflections, because of very strong power of noise and extremely weak signal of information. Intermediate dips could be treated fairly safely as true underground informations.

Field shot record contains velocity information and structural information mixed together as shown on Fig. IV-1-3, on the other hand, CDP family display after rearranging row data is free of structural effects with exception of too much complex structure case, and one can extract velocity information only and find out velocity distribution along vertical time.

Of course, CDP velocity has its dip factor of $1/\cos\theta$ as shown on Fig. IV-1-5, which is not negligible in (presumed) steep dip area like this.

Nevertheless, this velocity is usable for NMO correction (for stacking purpose only) without any modification. Then efforts were concentrated for picking lineups on CDP family in order to determine stacking velocity.

1-2 Velocity Information

Velocity information is to be acquired by checking that how reflection lineups on CDP

family display will fit theoretical travel time curves. If spread is shorter, range of theoretical curve which is considered to fit comes shorter, apparent probability of fitness comes bigger, and then judgement criterion will become very loose. Therefore, for extracting velocity information long spread data were used mainly. Velocity analyses on long spread data are based on constant velocity gather display with some reference to constant velocity scan display. Writers endeavoured to detect row reflection events which should be preferably recognized on displays by their bare eyes. However, because of extremely poor reflection signal quality it was very few to be able to read events which show reasonable velocity as waves penetrated into rock to some degree for carrying meaningful geological information back, in other words, do not show water velocity of 1450 m/s and nearby low velocities which should indicate no much penetration deeper than sea bottom.

Examples of picked events on constant velocity gather displays are shown on Figs. IV-1-6, IV-1-7, and IV-1-8. Picked velocity value plot on the figure of reflection time as ordinate and stacking velocity (practically same as V_{rms} : root mean square velocity) as abscissa is scattering very severely. Reasons of accuracy lack supposed are that signal strength might be very weak, and readable trace number of lineup is few and phases of waves are distorted because of clear disturbance by strong coherent noises like multiple refraction. Selected picked values only judged as comparatively reliable ones are plotted on Fig. IV-1-9, and following study was done on the considerations that velocity distribution of this area should fall within the scatterogram of these data.

Refraction first break velocity shown on CDP family display of long spread is mostly about 4 km/s, except west end portion of line T2 - AB (25 m). Particularly on far traces of some CDPs refraction velocity of 5 km/s or more was observed. According to these refraction observations rock velocity near sea bottom will be estimated to be fairly high. Assuming 1,450 m/s as water velocity, 100 ms as reflection time of sea bottom (equivalent to 72.5 m of sea depth), and 4 km/s as average rock velocity under seabottom, velocity function K shown on Fig. III-2-23 will be established. Because of no much contradiction with results of velocity analyses this K function was used mainly for final stack section.

Meantime, velocity inversion from Cretaceous limestone to Carboniferous clastic rocks was reported on sample measurements (M. Hosono et al, 1970). Taking account of this velocity inversion and assuming lower velocity clastic rock interval as long as possible, another velocity function T, lower velocity distribution than K, was calculated as shown on the same figure above, and used for one of preliminary stack sections on every line. Higher velocity

distribution than K, function H was also calculated and used. One more velocity function L, designed to meet prominent peaks of velocity spectra in low velocity region was established as shown on same figure, in spite of no much reality, but as reference. An example of L velocity stack section on T2 - AB (12.5 m) is shown on Fig. III-2-22, and multiple events are expressed as apparent horizontal structure.

1-3 Stack Section

Several different stack sections using different velocity functions were got as results. Final stack sections were made by means of applying broad band pass filter as wide as practically possible after stack using velocity function K in the case of short spread, velocity function V2 (judged temporarily as best) on T1-AB (25 m), and velocity function V4 (judged as above) on T2-AB (25 m). Final stack sections on long spread using velocity functions based on preliminary judgement do not mean necessarily and automatically best sections, in consequence, one must be referred to many other filtered and unfiltered sections for interpretation purposes. Fig. IV-1-9 depicts resolving power of velocity function applied on stacking. Referring to central curve of velocity function K lines of both sides show velocities incurring plus and minus 10 ms stacking error on both ends of spread along total length of streamer cable (active section); notice wide difference of range between short spread and long spread. If reflection wave of 50 cycle (period: 20 ms) is assumed, 10 ms error will cause attenuation of stacked output amplitude to about 64% (about $2/\pi$), and 20 ms error will cause zero output as calculated results. Accordingly, writers like to define temporarily the area within 10 ms stacking error (hatched on the figure) as allowable range of stacking when using some velocity function. Following this definition, almost velocity values got by velocity analyses mentioned above will fall onto the allowable range of short spread, and there should be no much fear that true reflection information may deteriorate badly after falling outside allowable range because of inadequate velocity function design. However, at the same time this means insufficient velocity selective operation, and consequently, on short spread data coherent noises of less penetration like multiple events might be more possible to survive. Therefore, long spread information, in which true reflection must be selected better, was interpreted first, and referring to geological considerations resulted from long spread study, short spread data were examined carefully.

1-3-1 T1-AB (25 m)

Events with inadequate velocity on this line must be cut out by stacking velocity filtering effect on long spread better than short spread case, however, if velocity function were not

chosen properly, true geological information rather than false one should be decayed by same effects. But, limiting to deeper portion more than 1 second of reflection time, almost all velocity values of events picked on constant velocity gather display will fall onto the allowable range as shown by hatch on Fig. IV-1-10, which is composite area applied on all velocity functions of T, K, and H; i.e., possibility of overlooking true reflection information could be eliminated sufficiently by means of careful checking on all T, K, and H stack sections. Though velocity function (V2: space variant, mentioned later) used on the final stack section of this line is somewhat higher than K at the part of more than 1 sec., this difference of velocity is thought not to affect very severely appearance of stack section.

Mute parameters selected first to cut off direct water wave on stack sections of T, K and H, produced overkilling of more than 1 sec on far trace of long spread, reduced fold number of shallower part upto 0.55 sec by half compared with short spread, and consequently deteriorated data quality more than short spread. For avoiding this bad side effects, first break suppression was limited to cut off sea bottom refraction first break only, and also automatic mute was restricted to work very moderately by keeping allowable stretch factor as large as possible. According to the modification of mute design like this, and special treatment of stacking velocity, shallow data were improved fairly well. But at the same time influences of shallow multiple energy remained to some degree after inevitably unsatisfactory elimination process.

Velocity function family which will produce 10 ms stacking error for each other neighbour on long spread are shown on Fig. IV-1-11. This family of eight velocity functions cover full range of picked event values on velocity analysis plot with enough margin even on shallower portion. An event between two neighbouring velocity functions should appear on stack sections using velocity functions on both sides of this event with some allowable attenuation, therefore, after comparing these stack results one can estimate velocity by which the event must build up most (i.e., V_{rms} of the event itself). This processing may be named as velocity function stack scanning, which means stack sections containing subsurface information is also a kind of velocity analysis tool. For comparing stack efficiency of each velocity function, eight stack sections are shown on Enclosure 16 (upto 1 sec. only). And also the final stack section with velocity function V2 is shown on Enclosure 15. On geological interpretation it is hoped that not only the final section but also stack scanning sections will be studied together, and event velocity can be checked by examing expressions of these stack sections.

Space variant velocity function stack scanning was also carried out, in which velocity functions were designed as follows. At CDP no. 48, nearly NE end of this line, and at CDP no. 626, nearly SW end of this line, velocity functions were as shown on Fig. IV-1-12 (higher velocity family depict CDP no. 626 value), and between them velocity change corresponds sea depth change only. It was assumed that interval velocity distribution in rocks is parallel to sea bed and no lateral change of each interval velocity exists. Stack sections of V1, V2, . . . , V5 were omitted in this report, after confirming that local part of them becomes very similar to same local part of VA, VB, . . . , VH on their appearance of wave form, if stacking velocity becomes very close to each other.

Stacking velocity applied on the final section was V2 up to 1 sec and on deeper portion this stacking velocity was extended on the assumption that the interval velocity of about 1 sec corresponding to V2 as V_{rms} does not change in deeper section.

1-3-2 T2-AB (25 m)

Data handling was done quite the same as previous section. Considering deeper part more than 1 sec only, there should not be much possibility of overlooking true reflection information, if stack sections of T, K and H velocities were checked carefully. Stacking velocity applied on the final section was V4 up to 1 sec, and this velocity was extended onto deeper section as mentioned above on T1-AB (25 m). This velocity is approximately same as H function on about 1 sec as results, and it is not confident to be best, consequently geological interpretation is recommended to be based on, and referred to other sections case by case.

Velocity function stack scanning by space variant velocity families of V1, V2, . . . , V5 was carried out on shallower portion less than 1 sec as same as T1-AB (25 m), for solving overmute problem and studying stacking velocity more in detail. Although this family was designed with subtle attention like narrow scanning interval and space variant, coverage was not enough as results (may not include full necessary range). Therefore, for studying more on velocity functions, it is recommended to restack data after applying velocity families of VA, VB, . . . , VH like on T1-AB (25 m), with taking stacking error magnitude into account. However, allocated resources were already critical, and this type of optional processing was not able to be done.

Space variant velocity functions of V1, V2, . . . , V5 at CDP no. 48, nearly east end of this line, and at CDP no. 712, nearly west end of this line, were as shown on Fig. IV-1-3 (higher velocity family depict CDP no. 48 value), and between them velocity functions were

interpolated as T1-AB (25 m) was treated. Therefore, stacking velocity for velocity function with same suffix number should be same on both lines at intersection, because same interval velocity of rock and same seabottom depth were assumed.

Comparing final sections of both lines, T2-AB (25 m) is with fairly higher velocity except far west part of deep sea area because V4 was applied on T2-AB (25 m) instead of V2 applied on T1-AB (25 m). Reason why V4 was elected as final mainly depends on very nice looking west dip event from about 250 ms at CDP no. 100 to about 350 ms at CDP no. 150, and for other events one does not see any significant superiority on V4 section than nearby sections. Accordingly one might be advised to study this final section with careful reference to other sections.

1-3-3 T2-AB (12.5 m)

Picking reflections on this line was carried out, using long spread data on T2-AB (25 m) as guiding index, because both lines located on quite same position. Although velocity function resolving should not be satisfactory because of short spread, judgement criteria were accustomed as follows. If event on stack section deteriorate on low velocity side of constant velocity stack display, one can feel safe, and, if event on stack section builds up on low velocity side, one must omit this event as false reflection. When there are energy concentrations on both sides of velocity display at similar reflection time with some depression between them, judgement might be; either,

- a) both events, low velocity noise like some kind of multiple energy and high velocity real reflection, exist,
- or
- b) low velocity noise only exists really, and high velocity energy concentration may show remainder of low velocity noise survived in side lobe area of stacking velocity filtering effect.

In such cases, suffered from double of interpretation, events were checked on CDP family display after NMO for searching raw reflection with reasonable moveout, even fragmental, by human eyes as best efforts. But unfortunately no reasonably reliable raw lineup could be recognized. According to calculation first side lobe is to attenuate event amplitude to about 21% (about $2/3\pi$). This magnitude of attenuation may not be enough to suppress noise sufficiently in such area of very strong multiple events like this.

1-3-4 T1-AB (12.5 m)

Judgement criteria of picking reflection by velocity information in addition to seismic

section appearance depend mainly on constant velocity stack display as same as previous section. Reflection quality was thought to be best of three short spread lines.

1-3-5 T3-AB (12.5 m)

Judgement criteria of picking reflection were as same as other short spread lines as mentioned on previous sections. If shallow flat events were considered as multiple refraction type noise, true geological information pickable becomes very few except deep events more than about two seconds. However, shallow flat events representing true geological information and multiple events are interfering each other at least locally, even if geological structure of shallow section looks like dipping gently to west in general. An example of possible interference of this kind on constant velocity stack display is shown on Fig. IV-1-14 (event of 555 ms and 4.5 km/s). In the case of suspected interference event search on CDP family after NMO by bare eyes was carried out without any remarkable success.

2. EXAMINATION OF REFRACTION RESULTS

2-1 Relation between Seafloor Velocity and Subsurface Topography

Concerning the dip of the seafloor, the subsurface topography is to be divided into three zones in the offshore Zonguldak area. Each of the zone distributes parallel to the coast, and it is summarized in Fig. IV-2-1.

- (1) Zone-1: The inshore area the slope has the dip of 2 to 3 degrees, and the boundary with the Zone-2 runs in accordance with the 60 meters water depth.
- (2) Zone-2: The feature of the second zone is very gentle having a dip of less than 1 degree, and the 80 meters water depth is generally representing the lower edge of the shelf.
- (3) Zone-3: Beyond the edge of the Zone-2, the third zone is steeply dipping toward the offshore Black Sea.

The relation between the obtained velocity shown in Fig. IV-2-2 and seafloor topography is as follows:

- (1)' Various velocities have been calculated in the area of the Zone-1.
- (2)' In the Zone-2, the lateral velocity change is very gentle with few exceptions.
- (3)' For the Zone-3, the velocity analysis could not sufficiently be made due to the lack of data and due to the deep water condition.

2-2 Comparison between Velocity Distribution and Gravity/Magnetics

Two gravitational high anomalies are observed in this area (ref. Fig. IV-3-1). The one, which is locating in the west of Zonguldak, identically corresponds to the high velocity zone (about 5.0 – 5.6 km/sec), where the limestone is exposing nearby peninsula. An another high gravity anomaly is situated at the north of Zonguldak, however, the corresponding high velocity zone is not observed. The relatively low velocity has been calculated in a portion of the gravitationally steep slope, fault or fault zone can be estimated by these phenomena.

A significant magnetic anomaly runs parallel to the coast line in the area off Kozlu, this seems to correspond to the zone-2 where less lateral velocity change is observed.

2-3 Comparison between Analyzed Velocity and Measured Velocity of Rock Samples

Table 8 shows the result of velocity measurement by means of Ultra-sonic method for rock samples (re-copied from Hosono et al. 1970), which are grouped by the geological series. Fig. IV-2-3 shows the relationship between density and P-wave velocity. The velocities of

Table 8 Result of Ultra-Sonic Wave Measurement on Rock Samples
(after Hosono, et al., 1970, Table 6)

System	Stage	Series	Rocks	Vp (km/sec) average & (range)	N	Density (g/cm) average	Sampling No.
Creta- ceous	Upper	Turonien	Andesite	3.3 (2.9-3.6)	3	2.39	12*1
	Lower	Apsien	Sand stone	3.7 (3.7)	1	2.58	7
			Lime stone	6.7 (6.3-7.1)	4	2.68	6, 11
		Barremien	Sand stone	—	—	—	—
			Lime stone	6.7 (6.4-6.9)	3	2.69	8
Carbo- niferous	West-falien	Karadon	Conglomerate Sand stone	3.2 (2.0-4.8)	6	2.44	9, 10
		Kozlu	Sand stone	3.8 (2.8-4.8)	7	2.59	2, 3, 4
	Namurien (upper)		Sand stone	3.4 (3.1-3.9)	4	2.61	1, 5

*1 location: 2 km SE of Göbô

N: Numbers of test sample

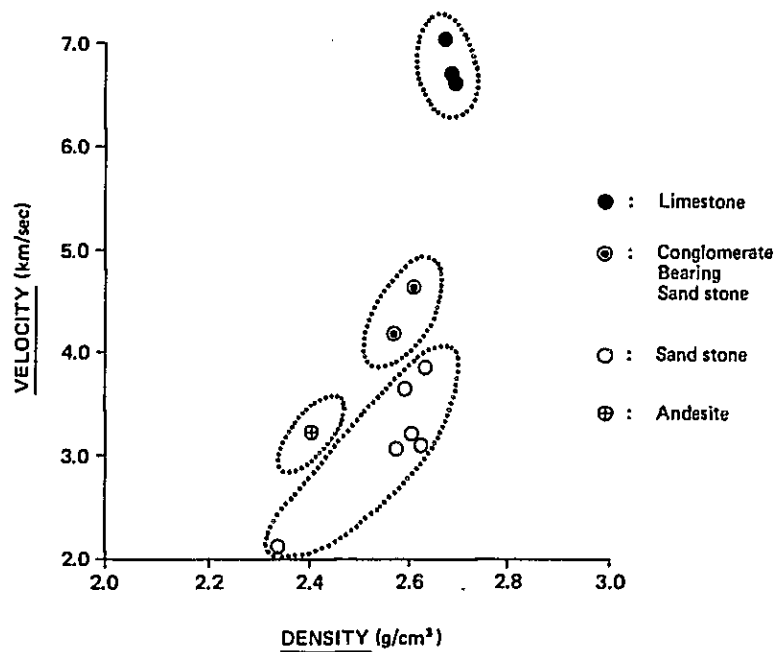


Fig. IV-2-3 Relation between Density and P-wave Velocity

limestones in the Apsien and Barremien series of lower Cretaceous show a very high value of about 6.3 – 6.7 km/sec, according to the result. The sandstone in the Kozlu Formation of Westfalien and the Apsien Flish have a velocity range of 3.7 – 3.8 km/sec. Relatively low velocities have been measured for the sandstone of the Namurien stage and Karadon formation of Carboniferous, of which the average is about 3.2 – 3.4 km/sec.

In comparison between these in-door data and calculated velocities based on the refraction data, the area where the velocity ranges from 3.6 to 4.0 km/sec seems to correspond to the area underlain by the sandstones in the Kozlu and/or Karadon formation of Carboniferous, or in the Apsien series of lower Cretaceous. However, due to the lack of data, the detail physical correlation should be reserved.

2-4 Comparison between Velocity Distribution and Geology

Local distribution of high velocity, 5.0 – 5.6 km/sec, nearby Kozlu may represent the outcrops of Cretaceous limestone at the seabottom. The low velocity zones which are dispersed throughout the survey line may indicate the existence of fault zones. In general, however, a conclusive geological interpretation could not be achieved because of sparsity of the velocity distribution. It is suggesting the necessity of the performance of the following tests or observations in the future to distinguish the apprehensible geology in the offshore zonguldak coal field.

- a) To conduct the additional geophysical survey with an appropriate line spacing.
- b) To accumulate the velocity measurements of the rock samples in laboratory by Ultrasonic wave method.
- c) To carry out the onland refraction seismics in the Zonguldak coal field.
- d) To carry out the sonic logging (using P-wave) in some drill holes located in the prospecting area.
- e) To continue the similar refraction analysis, as used in this subject, using reflection records acquired in 1977 and 1978 survey. In this case, the data from the lines of 62 (1977), Z-1 and Z-4 (1978) in the area shallower than 200 meters are probably useful.

3. EXAMINATION OF GRAVITY RESULTS

The result of the offshore gravity survey is shown as a Gravity map in Fig. IV-3-1 together with Magnetic profiles. For the convenience of examination, the residual gravity anomaly map (Normal structure) is overlaid on the geological map (Fig. IV-3-2).

3-1 Offshore Gravity Survey

The result of offshore gravity survey will be summarized as follows:

- 1) In general, the isogal (Bouguer) contour lines have a tendency to run parallel to the coast line.
- 2) These gravity values gradually decrease toward the Black Sea in the NW direction.
- 3) Local Bouguer anomalies occur at the both ends of T2-AB line.
- 4) In some portion, very steep gravitational gradient, i.e. dense gravity contour lines, were observed.

Events (1) and (2) may suggest the outer margin of the regional gravitational anticline observed in the onland area along the coast of the Black Sea. Also these events may suggest that general trend of the distribution of Palaeozoic to Cretaceous sediments are nearly parallel to the coast line in this area. The reliability of event (3) is considered to be low because these anomalies occurred at the end of survey line. The problem, whether these Bouguer anomalies have a geological meaning or not, still remains unsolved. From this point of view, positioning accuracy should be carefully checked in the future exploration survey. A steep gravitational gradient can be seen in the northern part of the peninsula, west of Zonguldak where a big gravitational gradient, about 1.5 mgal/100 m is recorded. The existence of a fault or a discontinuity between low and high density materials, such as limestone exposed nearby peninsula and its adjacent softer rocks may give an explanation of these events. To clarify the relationship between these gravitational events and their geological meanings, further data accumulations will be necessary.

3-2 Onland Gravity Survey

Fig. IV-3-2 illustrates the residual gravity anomalies obtained by the Running average method from the Bouguer Gravity map. This calculation was performed in an attempt to estimate the effectiveness of this method to the future offshore gravity survey in this area.

The main points on the residual gravity map are as follows:

- 1) The distribution of the formations from the Devonian to Lower Carboniferous is apparently expressed by the positive residual anomaly.

- 2) A fault at a distance of about 20 km southeast of Zonguldak in the direction of NE-SW can be seen more clearly on the residual gravity map than the Bouguer map.
- 3) The distribution of the coal mine shafts in Zonguldak coalfield nearly corresponds to the gravitational basin in the positive anomaly zone.
- 4) The shape of this gravitational basin appears to be identical with that of the Palaeozoic basin.
- 5) The general trend of the positive and negative anomalies on the residual gravity map in the area is in the direction of E-W while that of Bouguer gravity is of NE-SW.

From above mentioned results, it is apparent that gravity survey can be considered as one of the effective tool which can make specific and useful contributions to the overall exploration effort. The use of Bouguer anomaly, residual anomaly map and two dimensional simulation will improve the accuracy of the geological interpretation. Relationship between the gravitational basin and occurrence of coal bearing formation may suggest the importance of additional gravity survey in the area off Zonguldak coal field.

4. EXAMINATION OF MAGNETIC RESULTS

As a result of interpretation of offshore shipborne magnetic and onland aeromagnetic data, the following points are clarified.

- 1) In comparison with the data of onland geology, the total magnetic intensity appears to represent the distribution of tuff and volcanics of the Cretaceous.
- 2) In comparison with gravitational profile (A-A' in Fig. III-4-3) two separate magnetic anomalies on this profile tend to occur at the portion of gravitational flank.
- 3) A magnetic anomaly in the offshore area appears to be caused by the possible existence of Volcanics judging from the geological map.
- 4) Three dimensional simulation was applied to a magnetic anomaly which was observed by the previous survey in 1970, at the vicinity of No. 409 on T2-AB line, and obtained a model of magnetic body with the width of 1 to 1.5 kilometers and the depth of about 100 meters below sealevel.
- 5) A small magnetic anomaly on the NE part of line T1 may suggest the inner margin of this magnetic body.
- 6) In comparison with seismic velocity of uppermost layer obtained by refraction method, the magnetic anomaly occurs at a relatively low velocity zone ranging from 3.6 to 4.0 km/sec. Consequently, the velocity of magnetic body such as volcanics is likely lower than that of limestone.

5. PROBLEMS AND RECOMMENDATIONS IN POSITION FIXING

5-1 Problems in the Prepared Post-plots

The followings are observed in the post-mission documents which have been provided for the re-processing of the test survey.

- 1) Different map projection system is utilized for onland and offshore mapping.
- 2) Limited explanation has been given for the navigation log.
- 3) Insufficient specification is prepared for the post-plot processing.
- 4) Discrepancies were occurred in the numbering between positioning data and the geophysical records.
- 5) A few number of satellite updates have been made during shooting.
- 6) Due to the stand-alone line of T3, it is not possible to correlate with other lines.
- 7) Insufficient data are provided for the echo-sounding records.

5-2 Recommendations for the Future Offshore Exploration Survey

There is some apprehension to note the following advices, since the limited information were collected in the recalculation procedures. However, the following subjects can be raised in the offshore position fixing and the postmission data processing as the general consideration for the future activities.

- 1) If it is possible, the use of a high resolution radio navigation system (e.g. the TRISPONDER system) shall be employed for the primary positioning system.
- 2) During the survey, at least three shore stations shall be in continuous operation to provide positioning redundancy. The additional 3rd radio signal does not only allow to confirm the ship's position by real-time '3-way fixing', but also it will make possible easy station moves to get the adequate configuration of the radio navigation chains.
- 3) The Integrated Navigation System (NNSS + Doppler-Sonar) shall be used as a back-up positioning system in this case.
- 4) Any additional radio informations, for instance LORAN-C, shall generally be accepted if available.
- 5) The line control should be made according to preplots. The preplot lists*¹ of program lines and the suitable Lattice charts*², in which the program lines contained, must practically be used during the survey.

*1 Pre-plot lists: A set of calculation of distances from each shore station to the start point, end point and interperated points (usually every 200 meters) for the program line. This must be executed for the preparation of the pre-plot chart.

*2 Lattice Chart: A chart which has the group of circles or hyperbolas showing distances or travel-time differences from each shore station.

- 6) In this occasion, the use of onboard Trackplotter*³ is highly recommendable.
- 7) Detail logs shall be kept by onboard and shore station operators. The logs have to include the full of positioning log, navigation log, calibration log, and any other necessary notes on the system operations.
- 8) The reporting of these logs shall be submitted at the end of the survey by mobile and shore station operators.
- 9) The systematic computer management for the post-plot results must be carried out by using Magnetic Tapes. It shall be continued on filing updates in the subsequent surveys.
- 10) Using this tape file, the post-plot map must regularly be updated for the convenience of the geophysical interpretation.
- 11) The post-plot processing shall be made on every 4 shots (or 100 meters), and be displayed on the U.T.M. projection map.
- 12) The geophysical survey line must be intersected with the other lines.
- 13) The shore radio stations having accurate coordinates must be established at the good site for easy transportation and making best condigulation forward the survey area.
- 14) The echo-sounding equipment shall be well calibrated by for instance 'bar-check' method in the survey area.

The use of reliable navigation system and systematic postprocessing will guarantee to improve the quality of any geophysical parameters acquired at sea. It requires the intimate cooperation between the three onboard parties, namely the seismic group, the positioning group and the navigators of the ship. Furthermore, it is strongly required the close communication between the offshore surveyors and the onshore data processing team in order to achieve the high accurate position fix. The appropriate operation of the onboard equipment, the correct data logging and the post-processing at the computer center are, of course, the primary subjects in the offshore position fix.

*3 Track plotter: One of the onborad plotting system to display the real-time position of the sailing vessel. The pen is automatically followed by the radio signals. In this case if the survey program line has been given on the paper, the navigator can easily control the ship's course by altering the ship's heading to trace the line.

6. GEOLOGICAL AND STRUCTURAL INTERPRETATION IN THE PROJECT AREA

The summarized concepts on the geological and structural interpretation acquired from the compilation of the existing data and the present experimental offshore data are as follows:

1) General Geological Structure of the Objective Offshore Area

The general geological structure in the whole project area appears to be a monoclinial structure, which is dipping to the offshore, based on the results acquired from the seismic reflection and the gravity surveys and also from the sparker survey carried out in 1970.

2) Estimated Distribution of Volcanic Rocks

The clear magnetic anomaly is observed on each survey line as being recognized on every magnetic profile of the offshore survey line as shown in the Fig. IV-3-1.

There is a strong possibility that these magnetic anomalies may be connected with the tuffaceous and volcanic rocks which are surrounding the Zonguldak and Kozlu coal fields as shown in the geological map of Fig. IV-3-2.

As the seismic velocity at the seafloor in the magnetic anomalous area is in a steady range of 3.6 – 4.0 km/sec, the rock facies of these anomalous areas will be estimated those of a relatively low density.

Then, these anomalous areas would be apparently separated from the below-mentioned estimated distribution area of limestone.

3) Estimated Distribution of Limestone

The area being recognized to exhibit over 4.6 km/sec of seismic velocity at the southern part of the T1 survey line in the Fig. IV-2-2, distribution map of the seismic velocity at sea floor, will be identified as an extension of the limestone formation which exposes in the adjacent onland area of the project area.

As the P-wave velocity of limestone obtained from the Ultra-sonic measurement with the rock samples is in a range of 6.3 – 6.7 km/sec, which is a highest value among the test samples, it will be relatively easy to identify it from those of the other rocks.

This high seismic velocity area appears to correspond to the high gravity area. Then, there is a possibility on estimating the distribution of high density rocks in the area showing high seismic velocity.

And also, the correspondence between the physical property of rock and the rock kind may provide an important role to interpret the geology and structure of the project area. The further accumulation of background data would be desirable.

4) Structure Line (Fault)

The portion which has an estimated seismic velocity of below 3.0 km/sec by the refraction analysis seems to correspond to a fault or a disturbed zone. In the case the future exploration is programmed under more detail grid survey lines, these low seismic velocity zone will be quite effective to estimate the extension of the existing fault into the offshore and also to assume the scale of this estimated fault.

On the other hand, there is an example of estimated fault, in the northeast-southwest direction, at about 20 kms southeastern side of Zonguldak by the result of gravity analysis because there are so many cases that the area having a steep dipping of the residual gravity corresponds to the fault structure. Furthermore, there is a tail on estimating a fault structure designated by the low seismic velocity zone of refraction analysis at the west part of the T2-AB (12.5) survey line as shown at the eastern side of complex pattern of event visually identified in the seismic reflection profile of the same line.

5) Relation between the Distribution of Coal Mines and the Results of Gravity Analysis

It is quite interesting that there is a good correspondence between the distribution of coal mines and the gravitational basin shown by the residual gravity as shown in the Fig. IV-3-2 although the further investigation would be required.

6) . Deep Geological Structure on Reflection Profile

On every reflection profile reprocessed, a nearly flat event which could be a true reflection plane is recognized at about 2.5 to 3.0 second (about 4,000 m deep). It is, however, not yet interpreted at the moment and has to be clarified in the future investigation.